

Ph.D Programme in Complexity in Post-Genomic Biology

University of Torino – Italy



**VASCULAR BASEMENT MEMBRANE
GUIDES SPROUTING ANGIOGENESIS
THROUGH INTEGRIN A6 BINDING AND
LOCAL VEGFR2 PHOSPHORYLATION**

Dr. Giorgio Seano

Tutor: Federico Bussolino – IRCC – Turin (IT)

Referee: Holger Gerhardt – LRI – London (UK)

Rita Falcioni – IFO – Rome (IT)

Institute for Cancer Research and Treatment – Candiolo (TO)

Division of Molecular Angiogenesis

Laboratory of Cellular Migration

SUMMARY

<u>ABSTRACT</u>	3
<u>INTRODUCTION</u>	6
Angiogenesis: a multi-step process in embryos and in adult organisms	5
Vascular basement membrane in angiogenesis process	8
Integrins in angiogenesis	10
Dynamics of adhesive structures	12
Collective cell migration in sprouting angiogenesis.....	14
<u>MATERIAL AND METHODS</u>	17
<u>RESULTS</u>	25
Angiogenic growth factors induce $\alpha 6$ integrin expression in EC	24
Integrin $\alpha 6$ is required for in vitro angiogenesis and EC motility on basement membrane extract (BME).....	25
Down-regulation of integrin $\alpha 6$ in mouse aortic ring affects the endothelial sprouting ability in basement membrane extract gel	26
BM components control endothelial podosomes formation in a concentration-dependent manner	27
Integrin $\alpha 6$ is recruited in endothelial podosomes.....	29
Laminin controls podosome formation by decreasing integrin $\alpha 6$ localization to podosomes ...	30
<i>In vivo</i> down-regulation of integrin $\alpha 6$ affects podosomes formation in EC layer	31
BM directs migration of tip cells by localizing the activation of VEGF pathway in EC	33
<u>DISCUSSION</u>	36
Integrin $\alpha 6$, receptor for laminin, modulates sprouting angiogenesis	35
Laminin, through integrin $\alpha 6$ binding, blocks endothelial podosome formation and consequently BM degradation.....	36

Laminin directs the leading edge of sprouting angiogenesis.....37

FIGURES ***F1***

FIGURES LEGEND.....***39***

SUPPLEMENTARY FIGURES.....***SF1***

SUPPLEMENTARY FIGURES LEGEND.....***44***

REFERENCES.....***48***

ABSTRACT

In recent years, the basement membrane (BM) – a specialized form of extracellular matrix (ECM) – has been recognized as an important regulator of cell behavior, rather than just a structural feature of tissues. The functional study of integrins, transmembrane receptors for ECM, unveils important biological activities for BM in angiogenesis, the development of new vessels from preexisting ones. In particular, the integrin $\alpha 6$ subunit, heterodimerized with $\beta 1$ or $\beta 4$ integrin, is known to be receptor for laminins, the main component of BM. Integrin $\alpha 6$ and laminin mediates several biological activities in many morphological processes, but their precise role in angiogenesis has not yet been addressed.

We observed that both vascular endothelial growth factor (VEGF)-A and fibroblast growth factor (FGF)-2 strongly up-regulate $\alpha 6$ integrin in human endothelial cells (EC). Therefore, we studied the functional role of $\alpha 6$ integrin during angiogenesis by lentivirus-mediated gene silencing and blocking antibody. Cell migration and morphogenesis on BM extract, a laminin-rich matrix, was reduced in endothelial cells expressing low levels of $\alpha 6$ integrin. However, we did not observe any differences in type-I collagen matrices. Similar results were obtained in the aortic ring angiogenesis assay: $\alpha 6$ integrin was required for vessel sprouting into BM gels but not on collagen gels, as shown by stably silencing this integrin in the murine aorta.

Laminin and $\alpha 6$ integrin, in addition to playing a pivotal role in migration and morphogenesis activity, regulate the BM degradation capability by podosomes, specialized plasma-membrane microdomains that combine adhesive and proteolytic activities to spatially restricted sites of matrix

degradation. In fact, we observed that growing concentration of laminin decreased podosomes formation in EC *in vitro*. Therefore, we have investigated whether integrin $\alpha 6$ or integrin $\alpha 3$, the EC receptors of laminin, were recruited in podosomes. We demonstrated the presence of only integrin $\alpha 6$ in the ring structure that surrounds the podosome core, both in EC *in vitro* and in aortic vessels *in vivo*. Moreover, laminin decreased integrin $\alpha 6$ localization to podosomes in a concentration-dependent manner. To verify whether integrin $\alpha 6$ is functionally implicated in podosomes formation, we down-regulated integrin $\alpha 6$ *in vitro* and *in vivo*, by resulting in a strong reduction of endothelial podosomes number.

Finally, since ECM degradation and tip cells migration are directed towards BM, we investigated how BM establishes polarization of EC in aortic vessels. We set up a 3D sprouting model, called Mouse Aortic Sheet, by using explanted murine aortas cut along their long axis and embedded in ECM gel. Interestingly, into type-I collagen gel VEGF-driven angiogenic outgrowths sprouted only along the four borders of the aortic explants, while in BM extract gel Aortic Sheets showed sprouting outgrowths from the whole EC layer. These results suggested a local activation of EC layer as a consequence of BM contact. This hypothesis has been confirmed by the increase of localization of phospho-VEGFR2 and integrin $\alpha 6$ in basal side of *ex vivo* and *in vitro* EC as a consequence of addition of laminin.

In summary, we showed that the laminin- $\alpha 6$ integrin interaction guides angiogenesis *in vitro* and *ex vivo*, that BM degradation is driven by the amount of integrin $\alpha 6$ in endothelial podosomes and finally our results indicate that BM directs tip cells migration by localizing the activation of VEGF pathway in basal side of EC.

INTRODUCTION

Angiogenesis: a multi-step process in embryos and in adult organisms

From the earliest stages, the embryo develops in the absence of vascularization, receiving its nutrition by diffusion. In an ordered and sequential manner, however, the embryo rapidly transforms into a highly vascular organism, survival being dependent on a functional complex network of capillary plexuses and blood vessels.

“**Vasculogenesis**” refers to the initial events in vascular growth in which endothelial cell precursors (**angioblasts**) migrate to discrete locations, differentiate in situ and assemble into solid endothelial cords, later forming endocardial tubes (Fig. I). The subsequent growth, expansion and remodeling of these primitive vessels into a mature vascular network is referred to as “**angiogenesis**” (Fig. I). This process is characterized by a combination of sprouting of new vessels from the sides ends of pre-existing ones, or by longitudinal division of existing vessels with periendothelial cells (**intussusception**), either of which may then split and branch into precapillary arterioles and capillaries. Depending on the ultimate fate with respect to the type of vessel (artery, vein, capillary) and vascular bed, activated endothelial cells that are migrating and proliferating to form new vessels, forming anastomotic connections with each other, become variably surrounded by layers of periendothelial cells – pericytes for small vessels and smooth muscle cells for large vessels (“**vascular myogenesis**”) (Fig. I). During this dynamic period, extracellular matrix produced by mural cells and endothelial cells, serves to stabilize the network. Finally, further functional

modifications of larger arteries occur during “**arteriogenesis**” as a thick muscular coat is added, concomitant with acquisition of viscoelastic and vasomotor properties [3].

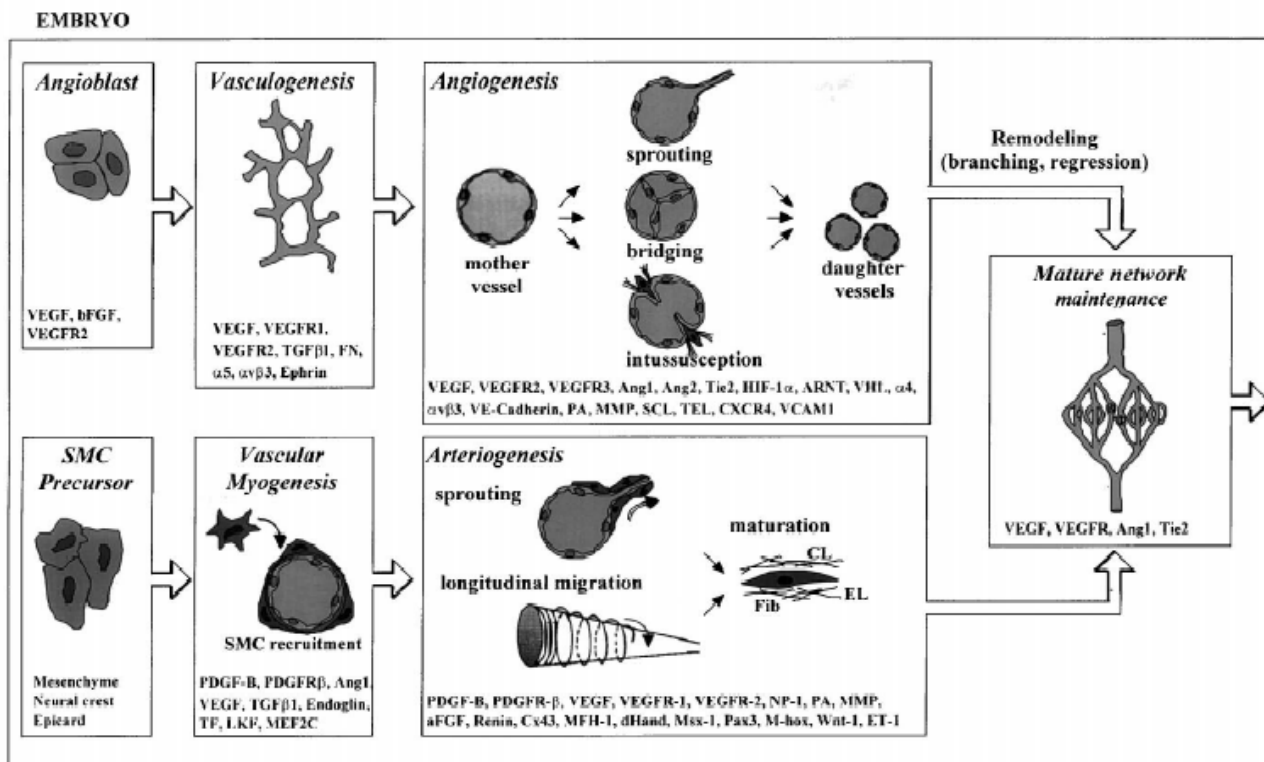


Figure I | **The multi-step morphogenesis process of blood vessel growth.** Endothelial precursors (angioblasts) in the embryo assemble in a primitive network (vasculogenesis), that expands and remodels (angiogenesis). Smooth muscle cells cover endothelial cells during vascular myogenesis, and stabilize vessels during arteriogenesis. CL, collagen; EL, elastin; Fib, fibrillin[3].

In particular, both in embryo development (as described above) and in adult organisms – in physiologic and pathologic conditions – **sprouting angiogenesis** is a multistep process whereby new blood vessels are formed from existing vessels [3, 5]. In response to angiogenic stimuli produced by microenvironment, it involves endothelial cell activation, interaction with adjacent basement membrane and degradation of the interstitial extracellular matrix, migration (sprouting) into the surrounding tissue, proliferation, alignment, tube formation, anastomosis, recruitment of parenchymal cells, and a return to quiescence (Figure II) [3, 5].

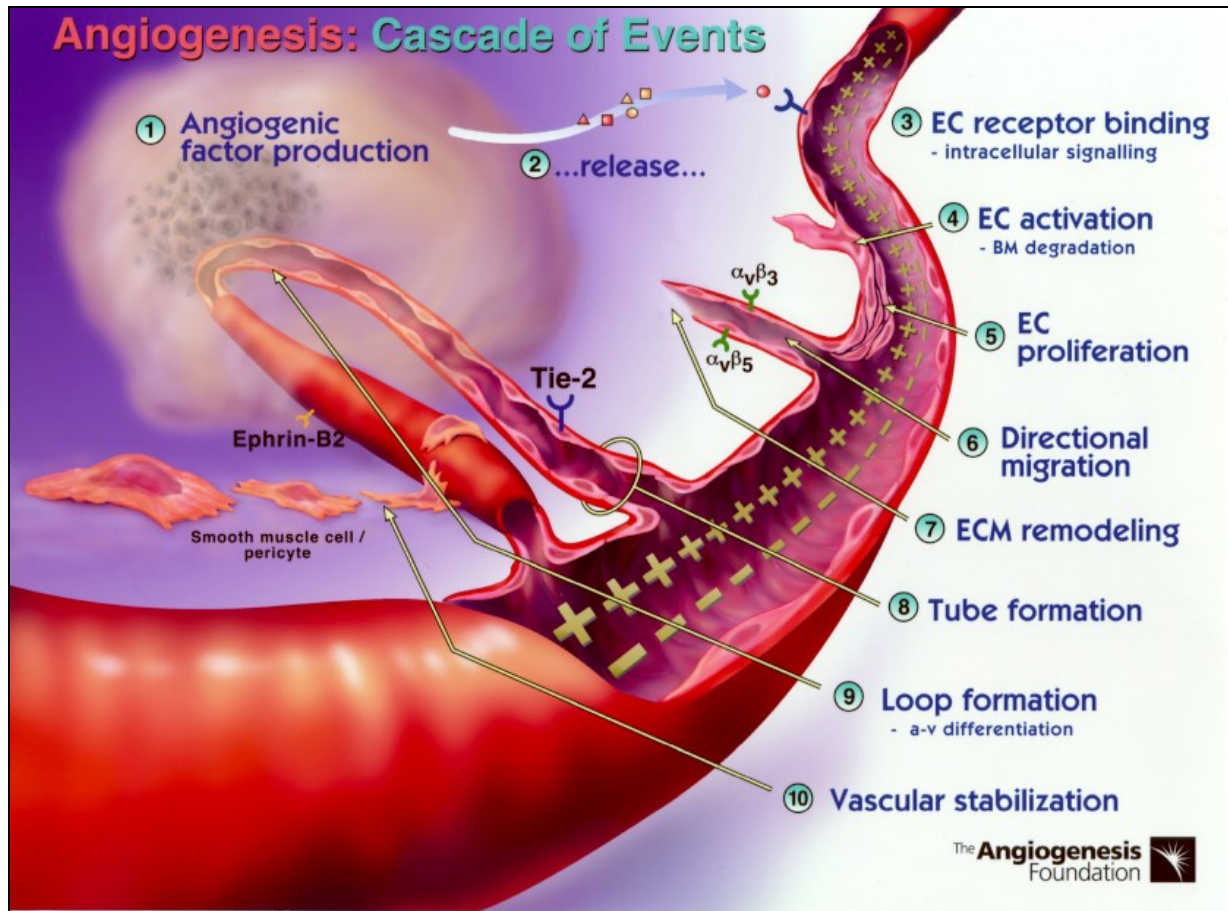


Figure II | **The Angiogenesis Process: How Do New Blood Vessels Grow?** (2009 by The Angiogenesis Foundation)

The process of angiogenesis occurs as an orderly series of events:

1. Diseased or injured tissues produce and release angiogenic growth factors (proteins) that diffuse into the nearby tissues.
2. The angiogenic growth factors bind to specific receptors located on the endothelial cells (EC) of nearby preexisting blood vessels.
3. Once growth factors bind to their receptors, the endothelial cells become activated. Signals are sent from the cell's surface to the nucleus.
4. The endothelial cell machinery begins to produce new molecules including enzymes. These enzymes dissolve tiny holes in the sheath-like covering (basement membrane) surrounding all existing blood vessels.
5. The endothelial cells begin to divide (proliferate) and migrate out through the dissolved holes of the existing vessel towards the diseased tissue (tumor).
6. Specialized adhesion molecules, called integrins ($\alpha_v\beta_3$, $\alpha_v\beta_5$), serve as grappling hooks to help pull the sprouting new blood vessel sprout forward.
7. Additional enzymes (matrix metalloproteinases, or MMP) are produced to dissolve the tissue in front of the sprouting vessel tip in order to accommodate it. As the vessel extends, the tissue is remolded around the vessel.
8. Sprouting endothelial cells roll up to form a blood vessel tube.
9. Individual blood vessel tubes connect to form blood vessel loops that can circulate blood.
10. Finally, newly formed blood vessel tubes are stabilized by specialized muscle cells (smooth muscle cells, pericytes) that provide structural support. Blood flow then begins.

Vascular basement membrane in angiogenesis process

In general, basement membranes (BM) separate the epithelium from the stroma of any given tissue. Additionally, BMs are usually found basolateral to epithelium, endothelium, peripheral nerve axons, fat cells and muscle cells. BMs are always in contact with cells, and their function is to provide structural support, divide tissues into compartments, as well as to regulate cell behavior [6]. Structurally, BM is an amorphous, dense, sheet-like structure of 50-100 nm in thickness that was identified by transmission electron microscopy [7]. It was observed to be similar to extracellular matrix (ECM) – a material that is usually present throughout the interstitium – but differed in density and was always associated with cells [4].

In particular, the **vascular basement membrane** is an important component of the vasculature, making up the “barrel” of every blood vessel and capillary. The inside of this barrel is lined by EC and the outside of this barrel is lined by pericytes – specialized smooth-muscle cells [7].

Vascular BM is composed of many different proteins that are produced by most cell types. The main components of BM are **laminin**, **type IV collagen**, and heparin-sulphate proteoglycans (HSPGs) such as perlecan and nidogen/entactin (Fig. III). Other proteins that are found in smaller amounts are type XV and XVIII collagens, fibulins, agrin, and SPARC/BM-40/osteopontin. BM self-assemble through a complex process that involves interaction with cell-surface proteins such as integrins to form a laminin network that is central to BM formation [8].

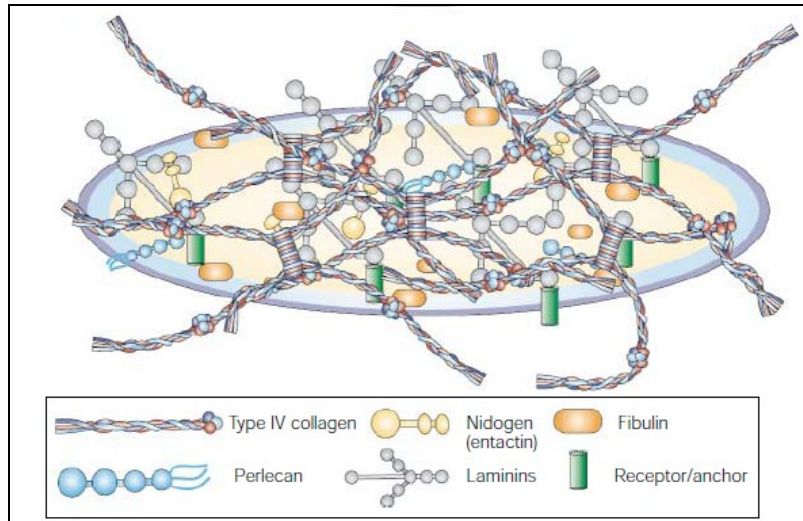


Figure III | **Schematic illustration of a BM scaffold formation outside the cell.** Most cells, except for immune cells, produce several forms of basement membrane (BM). Deposition of this polymer leads to association with type IV collagen network. Nidogen/entactin bridges the laminin polymer and the type IV collagen network, although some studies have indicated that direct interaction between the laminin polymer and type IV collagen network is possible. The other components of the BM interact with the laminin polymer and the type IV collagen network to organize a functional BM on the basolateral aspect of cells[4].

Vascular BM components are required for the initiation and resolution of angiogenesis. Although most of these components sustain the growth, survival and health of vascular endothelium, cryptic domains within these large proteins also possess anti-angiogenic activities. In this regard, matrix metalloproteinases (MMPs) and vascular integrins have emerged as key mediators of angiogenic and anti-angiogenic action mediated by the vascular BM.

Integrins were the first receptors identified to mediate the interactions between epithelial cells and BM components, such as laminin and type IV collagen [9]. Most of these initial studies were performed using the EHS-sarcoma-derived laminin-1 and type IV collagen. Several more recent studies have shown, however, that many other BM proteins can bind integrins and modulate cell behavior [10]. Integrins are a family of heterodimeric transmembrane glycoproteins mediating cell–cell and cell–ECM connections. The integrin family consists of eight β and 18 α subunits that assemble as heterodimers to form 24 distinct integrins [10]. A summary of the integrins and their binding sites in the main components of the BM is provided in Fig. IV.

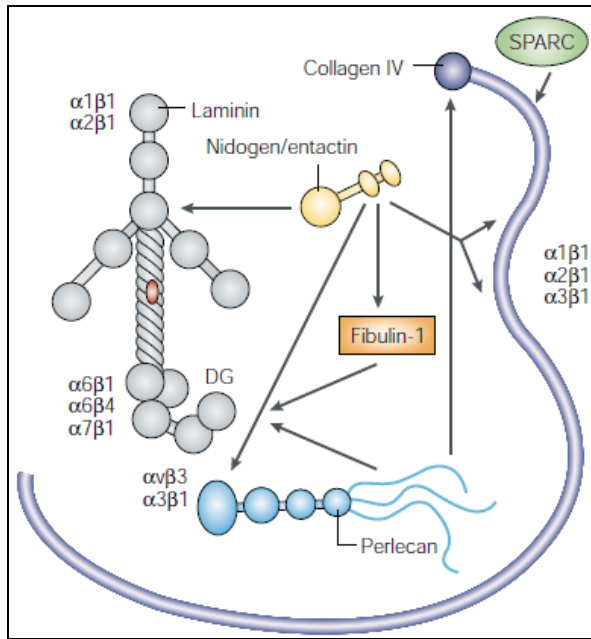


Figure IV | **Integrin binding sites on various BM molecules.** The basement membrane (BM) proteins laminin, collagen IV, nidogen/entactin, fibulin-1, perlecan and SPARC all bind integrins. The various integrins (that is, $\alpha1\beta1$, $\alpha2\beta1$, etc.) all bind to the regions indicated for the various BM components. The arrows indicate the sites at which the various BM proteins bind to each other. These sites were identified mainly using the EHS-tumour-derived BM molecules and proteolyzed fragments of these molecules. DG, dystroglycan[4].

Integrins in angiogenesis

As described above, the formation of new blood vessels depends on a finely tuned interaction between cells, extracellular matrix molecules, growth factors and proteases. The largest body of data has linked $\alpha v\beta3$ and $\alpha v\beta5$ integrins (both receptors for vitronectin and other extracellular matrix molecules) with blood vessel development [11]. Particular attention has been paid to the role of $\alpha v\beta3$ integrin in angiogenesis as it is prominent on proliferating vascular endothelial cells. In particular, proliferating endothelial cells express $\alpha v\beta3$, a key molecule for capillary formation [11]. Under steady-state conditions, integrin $\alpha v\beta3$ is not widely expressed. It is up-regulated on cytokine-activated endothelial as well as on vascular cells within malignant tumors. Blockade of $\alpha v\beta3$ integrin with monoclonal antibodies or low-molecular-weight antagonists inhibits blood vessel formation in a variety of *in vivo* models, including tumor angiogenesis and neovascularization during oxygen-induced retinopathy [11]. A single small-molecule inhibitor of both $\alpha v\beta3$ and $\alpha v\beta5$ integrins inhibited tumor angiogenesis in animal models [12].

In contrast with these inhibitor studies, genetic studies have suggested that integrin $\alpha v\beta 3$ is not required for angiogenesis. For example, some mice lacking αv integrins exhibit extensive developmental angiogenesis [13]. Most αv -null embryonic mice develop normally until embryonic day 9.5 whereupon 80% of mice exhibit placental crises; approximately 20% of αv -null mice survive to birth but die just after birth with extensive brain hemorrhages [13]. Similarly, only 50% of $\beta 3$ -null mice are viable and fertile; in these mice, developmental angiogenesis, including postnatal neovascularization of the retina, appears to be $\beta 3$ independent [14].

A further complication in the knowledge of $\alpha v\beta 3$ functions was the failure of anti-angiogenic clinical trial with $\alpha v\beta 3$ and $\alpha v\beta 5$ inhibitors [15]. Only recently *in vivo* evidences have been presented in which low (nanomolar) concentrations of RGD-mimetic $\alpha v\beta 3$ and $\alpha v\beta 5$ inhibitors can paradoxically stimulate tumor growth and tumor angiogenesis, as seen in clinical trials. It has been shown that low concentrations of these inhibitors promote VEGF-mediated angiogenesis by altering $\alpha v\beta 3$ integrin and VEGFR2 trafficking, thereby promoting endothelial cell migration to VEGF [15].

Additional ECM-binding integrins that play critical roles in angiogenesis include $\alpha 1\beta 1$ and $\alpha 2\beta 1$ which bind laminin and collagen. In normal animals, VEGF-A treatment up-regulates expression of both $\alpha 1\beta 1$ and $\alpha 2\beta 1$ on vascular endothelial cells [16].

Finally, the **integrin $\alpha 6$** can form heterodimers with both $\beta 1$ and $\beta 4$ subunits. Integrin $\alpha 6\beta 1$ can bind many ECM proteins such as laminin, thrombospondin, and CYR61, whereas $\alpha 6\beta 4$ primarily binds laminin. Importantly, the $\beta 4$ integrin subunit and its ligand laminin, is expressed by human and murine tumor endothelium [17, 18]. Mice with genetic deletions of the $\beta 4$ or the $\alpha 6$ subunit do not exhibit overt vascular defects but die immediately after birth, in part due to severe skin blistering caused by passage through the birth canal [19, 20]. However, it is not yet clear what role integrin $\alpha 6$ plays in physiological and pathological angiogenesis.

invadopodia could be involved in matrix degradation and invasion, whereas focal adhesions are rather associated with adhesion and matrix remodeling such as fibronectin fibrillogenesis [21].

Tangential cell–matrix contacts: in cultured cell, a family of focal adhesion-related structures has been identified and named **focal complexes**, **focal adhesions**, and fibrillar adhesions [22]. Focal complexes are 0,5- to 1- μm dot-like contacts localized along the lamellipodia. These structures are not connected to stress fibers although they have been shown to be linked to the actin network. Moreover, they do not contain Zyxin, by suggesting that they are subjected to moderate mechanical tensions. Focal complexes mature into focal adhesions, the elongated 3- to 10- μm structures associated with stress fibers. Focal adhesions are the best characterized type of focal adhesion-related structures (Figure V) [2].

Perpendicular cell–matrix contacts: Podosome-type adhesions (PTA) are found in migratory and invasive cells [21]. **Podosomes** and **invadopodia** are actin-rich membrane structures (with dimensions ranging from 0,5 to several μm) that form close contact with the surrounding substrate. Current convention is to use the term podosome for the structures found in normal cells (such as monocytic cells, endothelial cells and smooth muscle cells) and in Src-transformed fibroblasts, and invadopodium for the structures found in cancer cells. Podosomes are specialized plasma-membrane actin-based microdomains consisting of a core of actin filaments associated with the Arp-2/3-based actin polymerization machinery and surrounded by a ring of vinculin, talin, paxillin and integrins. They can be distinguished from other focal adhesions complexes by the presence of “podosomal markers”, such as gelsolin, cortactin, dynamin 2 and WASP/NWASP proteins (Figure V). In addition, podosomes are enriched with metalloproteinases, which endow them with matrix-degradation activities. In physiological settings, podosomes form spontaneously in certain cells such as macrophages and immature dendritic cells, which share the common feature of travelling across tissue boundaries. Podosome-related structures named invadopodia assemble in cultured cells

transformed by the viral src oncogene and in melanoma or carcinoma in response to oncogenic signals [23].

Collective cell migration in sprouting angiogenesis

Cell migration is the crucial process for the formation of new vessels from preexisting ones, in physiology and pathology. Cell migration at the single-cell level has been studied extensively over many decades [24, 25]. In brief, migration of a typical cell can be described as follows:

The cell expands by making protrusions, generally driven by actin polymerization; these can be large lamellipodia, small filopodia, and combinations thereof. Local cortical blebbing can also drive cell expansion. The cell needs adhesion to, and traction on, the substratum. Integrin-based focal adhesions, or related contacts with the extracellular matrix (ECM), can support traction. If the substrate is other cells, cell-cell adhesion molecules can mediate these contacts. Finally, the cell exerts a pulling force to translocate the cell body forward and also retracts its rear [24, 25].

Although, much is known about single-cell migration, the type of cell movement that better represents sprouting angiogenic process is collective cell migration [26, 27].

As reviewed by Friedl and Gilmour, three hallmarks characterize collective cell migration. First, the cells remain physically and functionally connected such that the integrity of cell–cell junctions is preserved during movement [28]. Second, multicellular polarity and “supracellular” organization of the actin cytoskeleton generate traction and protrusion force for migration and maintain cell-cell junctions. Third, in most modes of collective migration, moving cell groups structurally modify the tissue along the migration path, either by clearing the track or by causing secondary ECM modification, including the deposition of a basement membrane [27].

Collective cell migration involved in sprouting angiogenesis is guided by three cellular components with specialized functions (Fig. VI):

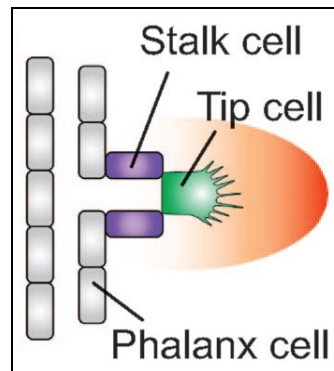


Figure VI | **Vascular sprouts are guided by endothelial tip cells.** Schematic representation of a tip cell (green) extending filopodia toward an angiogenic stimulus (red gradient), followed by stalk cells (purple), while phalanx cells (gray) remain quiescent[3].

The first and, to a certain extent, the most undertaking cell in a vessel branch is the “tip cell”, which leads the way. With their continuously searching filopodia, these tip cells sense and respond to guidance cues in their microenvironment, similar to how an axonal growth cone in the nervous system [29]. It is therefore not surprising that several classes of molecules and principles, used by navigating axons or epithelial cells, are evolutionary conserved and shared, and even might have been coopted by the migrating endothelial tip cell [30].

“Stalk cells” trail behind the tip cell and elongate the stalk of the sprout; they proliferate, form junctions, lay down extracellular matrix, and form a lumen. As reviewed by Phng and Gerhardt, endothelial tip and stalk cells differ in their gene expression profile; tip cells express PDGFR β , Dll4, Unc5b, VEGFR2, and Flt4 more strongly than stalk cells (Fig. VII). These differences are detectable only in mRNA levels. It is important to note that no single gene identified thus far can serve as a unique marker of tip cells. Nevertheless, these quantitative differences in gene expression support the idea that tip and stalk cells have specialized functions during sprouting angiogenesis [1].

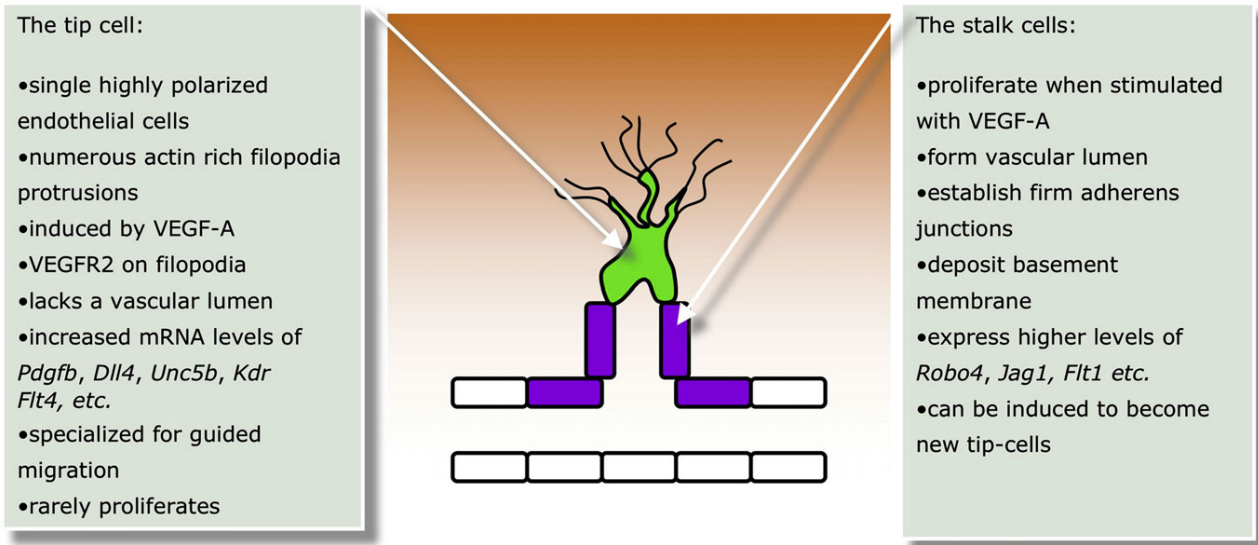


Figure VII | **Phenotypic and Molecular Differences between Endothelial Tip and Stalk Cells.** Tip cells (green) head each vascular sprout stimulated by an extracellular VEGF-A gradient (orange), and the following endothelial cells (purple) form the lumenized stalk[1].

“Phalanx cells” are the most quiescent EC, lining vessels once the new vessel branches have been consolidated; they form a smooth cobblestone monolayer and are aligned as in a phalanx formation of the ancient Greek soldiers, are covered by pericytes, stick to each other via tight junctions, are embedded in a thick basement membrane, and stay foot [26]. These cells are engaged in optimizing blood flow, tissue perfusion, and oxygenation [31]. Tip, stalk, and phalanx ECs each have a specialized function in vessel branching.

MATERIALS AND METHODS

Cell culture and reagents

Human umbilical vein endothelial cells (EC) were isolated from umbilical cord vein, characterized and grown as previously described [32]. In all experiments, EC were used between passages two and five. 293T (ATCC® CRL-11268), and Hela (ATCC® CCL-2) cell lines were obtained from American Type Culture Collection and maintained as frozen stock. These repositories authenticate all human cell lines prior to accession by DNA fingerprinting. All experiments were performed on cell lines that had been passaged for <6 month after thaw and cultured in DMEM (Cambrex) supplemented with 10% FCS, 2 mM L-glutamine (Cambrex), and antibiotics.

Rat monoclonal function-blocking antibody against integrin $\alpha 6$ (GOH3), VEGF-A, FGF-2 and Angiopoietin-1 were obtained from R&D System. Laminin (Sigma) and type IV collagen (BD Biosciences) were isolated from Engelbreth-Holm-Swarm murine sarcoma basement membrane.

Quantitative RT-PCR

RNA was prepared using TRIzol (Invitrogen) according to the manufacturer's instructions. Expression of integrins was analyzed by quantitative real-time reverse transcription-PCR (qRT-PCR) using TaqMan Gene Expression Assay (humanITGa6 Hs00173952; humanITGb1 Hs00236976; mouseITGa6 Mm00434375; mouseITGa5 Mm00439797; mouseITGb3 Mm004439797; VEGFR2 Mm01222419) from Applied Biosystems. Integrin mRNA quantities were analysed in triplicate, normalised against human glyceraldehyde-3-phosphate dehydrogenase (GAPDH) or mouse TATA-

binding box protein (TBP) as control genes, and expressed in relation to calibrator samples. PCR reactions were performed on the ABI Prism 7900 HT Sequence Detection System (Applied Biosystems) using the fluorescent TaqMan methodology. Results are expressed as relative gene expression using the $\Delta\Delta C_t$ method. The relative quantification method employed was based on the following arithmetical formula $2^{-\Delta\Delta C_t}$, where $\Delta\Delta C_t$ is the normalized signal level in a sample relative to the normalized signal level in the corresponding calibrator sample.

Cytofluorimetric analysis

Cells were trypsinized and then incubated with 5 $\mu\text{g/ml}$ of mouse α -Integrin $\alpha 6$ mAb (4F10, Santa Cruz Biotechnology), rat α -Integrin $\alpha 6$ (GOH3, Serotec), and mouse and rat IgG for 30 min. After three washes with PBS 1% BSA, cells were incubated with 2.5 $\mu\text{g/ml}$ R-phycoerythrin anti-mouse or donkey anti-rabbit Alexa Fluor 488 antibody (Southern Biotechnology Associates or Invitrogen) for 30 min. After final washes with PBS, samples were fixed with PBS 2% PAF, acquired by CyAn™ ADP (Dako), and analyzed using Summit 4.3 (Dako).

Immunoprecipitation and immunoblotting analysis

Subconfluent EC were cultured with 10% FCS M199 for 12h and either unstimulated or stimulated with 20 ng/ml VEGF-A or 10 ng/ml FGF-2 for 24 and 48h. Cells were transferred to ice, labelled with Biotin (Pierce), washed three times with cold PBS containing 1 mM Na orthovanadate, and lysed in RIPA-modified buffer containing 20 mM Tris, pH 7.2, 150 mM NaCl, 1% Triton X-100, 0.5% Na deoxycolate, 0.1% SDS, 5 mM EDTA, and protease and phosphatase inhibitors (50 $\mu\text{g/ml}$ pepstatin, 50 $\mu\text{g/ml}$ leupeptin, 10 $\mu\text{g/ml}$ aprotinin, 1 mM PMSF, 100 μM ZnCl₂, 1 mM Na orthovanadate, and 10 mM NaF). After centrifugation (15 min at 10,000g), supernatants were precleared by incubation for 1 hour with protein G-Sepharose (GE Healthcare). Equal amounts of

proteins for each sample were incubated with rat α -ITG α 6 (GOH3) for 2 hours, and immune complexes were recovered on protein G-Sepharose. Beads were washed four times with lysis buffer and detected by immunoblotting: proteins were separated by SDS-PAGE electrophoresis, transferred to polyvinylidene difluoride (PVDF) membrane (Millipore), incubated with Streptavidin-HRP and, after stripping, with mouse anti- β 1 integrin (JB1B, Abcam), and visualized by the ECL system (GE Healthcare).

In vitro morphogenesis assays

For in vitro morphogenesis on basement membrane extract (BME) – Matrigel (BD Biosciences) or Cultrex (Trevigen) – were added to each well at concentration of 8 mg/ml and incubated at 37°C for 30 minutes to allow gel formation. EC (2×10^4 /well) were plated onto BME in presence of 20 ng/ml VEGF-A and 10 ng/ml FGF-2. After 8h of incubation in 5% CO₂ humidified atmosphere at 37°C, cell organization was examined.

Collagen sprouting assay was performed as previously described [33]. Briefly, EC spheroids were suspended in medium with or without 20 ng/ml VEGF-A, and mixed with an equal volume of diluted collagen solution (0,6 mg/ml), collagen solution plus 50 μ g/ml of Laminin or BME gel (8 mg/ml). Antibodies were applied before gel solidification and administered in medium with a final concentration of 20 mg/ml. Capillary-like sprouts were examined with inverted-phase contrast microscope (Leica Microsystem, Heerbrugg, Switzerland) and photographed. Lengths of the capillary-like structures were quantified with the imaging software winRHIZO Pro (Regent Instruments Inc.).

Immunostaining

EC plated on coated coverslips or whole-mount tissue pieces were equilibrated in TBS and fixed with 3,7% PAF or Zn-Fixative Buffer. Primary antibodies - rat anti- $\alpha 6$ integrin (GOH3), goat anti- $\alpha 3$ integrin (Chemicon), mouse anti-vinculin (BD Biosciences), mouse anti-cortactin (Millipore), rabbit anti-src (Cell Signaling Technology), rat anti-CD31 (BD Biosciences), rabbit anti-VEGFR2 mAb and anti-phosphoY1175-VEGFR2 (Cell Signaling Technology) - were diluted in PBS plus 25% blocking solution and incubated overnight at 4°C in a humidified chamber. Sections were washed with PBS and incubated for 30 min at room temperature with secondary antibodies. Finally, they were stained by Alexa Fluor conjugated phalloidin (Molecular Probes) for 20 min. Whole-mount tissue pieces or coverslips were mounted in mounting medium that contained DAPI (Vector Laboratories, Burlingame, CA) and analyzed using a confocal laser-scanning microscope (TCS SP2 with DM IRE2; Leica) equipped with 20 \times , 40 \times and 63 \times /1.40 HCX Plan-Apochromat oil-immersion objective. For TIRF microscopy, after automatic Leica proceeding of lasers auto-alignment, we analyzed mounted coverslips with a deepness reflection of 90 nm (Leica Microsystems LAS AF 6500/7000).

Confocal stack images for apical:basal analysis were digitally post-processed with background subtraction and blind deconvolution algorithms with Imaris, Autodeblur or ImageJ.

shRNA sequences and lentiviral preparation

Lentivectors carrying short hairpin RNAs (shRNA) sequences against human and mouse Integrin $\alpha 6$ or a scramble sequence (used as control) derive from the RNAi Consortium library (Sigma-Aldrich). All viruses were produced as described in the TRC shRNA guidelines [34]. The efficiency of gene silencing was analyzed with cell infection followed by FACS analysis with specific anti-Integrin $\alpha 6$ Abs.

Adhesion assay

20,000 ECs were re-suspended in 0,2 ml of M199 with 20 ng/ml VEGF-A and 10 ng/ml FGF-2, plated on 96-well microtitre plates (Costar) coated with either collagen (Sigma), BME (BD Biosciences) or laminin (Sigma), incubated for 30 minutes at 37°C, washed two times with PBS, fixed in 8% glutaraldehyde, and stained with 0.1% crystal violet, 20% methanol. 595 nm absorbance was obtained dissolving crystal violet from stained cells with 10% acetic acid.

Migration assay

EC were seeded at high density on 10 µg/ml Collagen or BME-coated 24-well plates; cells were wounded by dragging a plastic pipette tip across the cell surface and 20 ng/ml VEGF-A and 10 ng/ml FGF-2 were added to medium. In experiments of functional blocking Ab treatment, the final concentration of GOH3 or rat IgG is 10 µg/ml. Wound closure response was followed, and quantified by inverted-phase contrast time-lapse microscopy (Leica Microsystems LAS AF 6500/7000).

Mouse Aortic Ring angiogenesis assay

The mouse Aortic Ring assay was performed as previously described [35] with modifications. Briefly, thoracic aortas were removed from 8-12 weeks-old wild type C57/BL6 mice (Charles River) and fibro-adipose tissue was dissected away. Aortas were sectioned in one mm-long aortic rings and incubated for 2 days in serum-free medium with antibiotics, polybrene and lentiviral supernatant. 48-well culture dishes were coated with 100 µl of type I collagen (from rat tail, Roche) or BME and allowed to solidify. These were then sealed in place with an overlay of 70 µl of Collagen or BME and covered with 300 µl of Endothelial Basal Medium (EBM®, Clonetics) 5% FCS or M199 10% FCS with VEGF-A (final concentration 20 ng/ml) and FGF-2 (final concentration 10 ng/ml). In the case of functional blocking Ab treatment, the final concentration of GOH3 or rat IgG was 10 µg/ml.

Tubular structures were examined with inverted-phase contrast microscope (Leica Microsystem, Heerbrugg, Switzerland) and photographed. Lengths and projected areas of the capillary-like structures were quantified with the imaging software winRHIZO Pro (Regent Instruments Inc.).

Cell and aortic vessel podosome stimulation

EC were seeded for 2 hours in M199 20% FCS on coverslips, coated by 1% porcine gelatin and saturated by PBS 1% BSA. Cell were starved with M199 serum-free for 1 hour and then stimulated with M199 10% FCS plus 60 ng/ml of phorbol-12-myristate-13-acetate (PMA), fixed, stained with anti-cortactin Ab and phalloidin and analyzed with confocal microscopy. In experiments of functional blocking Ab treatment, the final concentration of GOH3 or rat IgG is 20 µg/ml.

Aortic vessels were explanted as described above. After cleaning from fibro-adipose tissue, murine aortas were cut along their long axis and incubated for 24 hours in serum-free medium with antibiotics. Finally, aortic segments were stimulated with M199 10% FCS plus 60 ng/ml of PMA, fixed, stained with anti-cortactin Ab and phalloidin and analyzed with confocal microscopy.

Mouse Aortic Sheet Sprouting Assay

The mouse Aortic Sheet sprouting assay was performed as previously described in mouse Aortic Ring with modifications. To obtain aortic sheets, murine aortas were cut along their long axis. Then Aortic Sheets were put into a gel drop – type I collagen (1,5 mg/ml, from rat tail, Roche) with or without addition of laminin or BME (Matrigel, BD) – before solidification on glass chamber slide (Lab-Tek® Chamber Slide™ System, Electron Microscopy Sciences). This thin preparation, which allows live *ex vivo* visualization and whole-mounted immunofluorescence, was covered with 300 µl of Endothelial Basal Medium (EBM®, Clonetics) 5% FCS with VEGF-A (final concentration 30

ng/ml). Finally, aortic sheet cultures were fixed, stained with anti-CD31 Ab and phalloidin and analyzed with confocal microscopy.

RESULTS

Angiogenic growth factors induce $\alpha 6$ integrin expression in EC

By microarray gene expression analysis we found that mRNA expression of $\alpha 6$ integrin was significantly up-regulated in human EC upon stimulation with VEGF-A and FGF-2 (data not shown). We confirmed these results by performing qRT-PCR experiments. EC stimulated for 24h with VEGF-A and FGF-2 increased the expression level of integrin $\alpha 6$ by 13- and 10-fold respectively compared to unstimulated cells (Fig. 1A). In the same experimental conditions, angiotensin-1 induced a limited up-regulation of $\alpha 6$ integrin mRNA (Fig. 1A).

We examined the surface expression of $\alpha 6$ integrin by flow cytometry analysis observing an increase of $\alpha 6$ positive cells after 24 hours of stimulation with VEGF-A and FGF-2 (Fig. 1B). Interestingly, in the absence of growth factors, approximately 20% of EC expressed detectable levels of $\alpha 6$ integrin, while upon treatment with angiogenic growth factors for 48 hours almost 80% of the cells became positive (Fig. 1B). Although $\alpha 6$ can form both $\alpha 6\beta 1$ and $\alpha 6\beta 4$ heterodimers, human cultured EC do not express detectable levels of integrin $\beta 4$, therefore only the $\alpha 6\beta 1$ heterodimer is expressed (data not shown and [17]). While immunoprecipitation experiments indicated that both subunits of $\alpha 6\beta 1$ integrin were up-regulated upon treatment with VEGF-A and FGF-2, the protein and mRNA level of total $\beta 1$ integrin was not modulated by growth factor stimulation. (Fig. 1A,C). Therefore, the amount of $\beta 1$ associated with $\alpha 6$ was only dependent on the $\alpha 6$ integrin expression, although some differences in the association ratio have been observed (Fig 1C and S1).

These results suggest that $\alpha 6$ integrin was highly expressed on activated EC, but nearly absent on quiescent EC.

Integrin $\alpha 6$ is required for *in vitro* angiogenesis and EC motility on basement membrane extract (BME)

To examine whether $\alpha 6$ integrin was directly involved in the angiogenic process, we inhibited integrin function by blocking antibody and gene silencing. We assessed whether $\alpha 6$ integrin is required for *in vitro* angiogenesis by using the endothelial tube formation assay in which EC, placed on BME gel in the presence of angiogenic factors, self-organize into structures morphologically similar to capillaries.

The addition of an $\alpha 6$ integrin-blocking antibody, completely inhibited the *in vitro* tube formation (Fig. 2A). Moreover, integrin $\alpha 6$ was stably down-regulated in EC by shRNA lentivirus transduction, selecting two shRNAs that were able to silence more than 50% of the membrane protein compared to a scrambled shRNA (shScr1) (Fig. S2). In order to rescue the integrin expression, silenced EC were transduced with murine $\alpha 6$ integrin cDNA, which led to expression of $\alpha 6$ at levels similar to wild-type cells (Fig. S2B). As shown in Figures 2B, EC silenced with either shITGA6_4 or shITGA6_5 failed to form tubular structures while shITGA6_4 EC expressing murine ITGA6 displayed a network similar to that of shScr1 EC.

These results were not confirmed in another *in vitro* angiogenesis model, the collagen sprouting assay. In this model, spheroids of EC, embedded in collagen type-I gel, sprout when stimulated by VEGF-A or FGF-2 forming tubular structures. EC spheroids with reduced ITGA6 expression or treated with the $\alpha 6$ blocking antibody, sprouted at same extent as spheroids transduced with shScr1 or in presence of rat IgG (Fig. 2C and S3).

Nevertheless, the addition of laminin, an $\alpha 6$ integrin ligand, to collagen gel, increased the sprouts formation while the blockade of $\alpha 6$ integrin significantly reduced the sprouts length (Fig. 2C). Similar results have been obtaining embedding spheroids in BME gel in which EC formed mainly cord-like rather than tubular-like structures (Fig. S3). Therefore, $\alpha 6$ integrin regulates the *in vitro* angiogenesis in presence of ECM-containing laminin but appears irrelevant when unbound to its specific ligand.

Although it is conceivable that these effects were consequence of loss of adhesion strengthening, experiments on different ECM indicated that adhesive ability of $\alpha 6$ integrin-silenced cells was unaffected on collagen and BME, while was only partially reduced on laminin (Fig S4A). To examine instead whether $\alpha 6$ integrin was involved in EC migration, we performed a wound/scratch assay on BME and collagen matrix. EC plated on BME, scratched and treated with anti- $\alpha 6$ blocking antibody displayed a significantly decreased motility compared to EC treated with control IgG (Fig. 3A). Similar results were obtained with silenced cells, which showed reduced migration ability that was rescue by re-expression of murine $\alpha 6$ integrin cDNA (Fig. 3B). In contrast, the absence of integrin $\alpha 6$ did not interfere in EC motility on collagen type-I (Fig. S4B). As expected, most of the focal adhesions at the leading edge of cell migrating on BME contained $\alpha 6$ integrin, suggesting its active role during the directional motility, while it was not recruited on collagen-induced focal adhesions (Fig. 3C-D).

Down-regulation of integrin $\alpha 6$ in mouse aortic ring affects the endothelial sprouting ability in basement membrane extract gel

In order to exclude that levels of $\alpha 6$ integrin solely affect the angiogenic response of cultured EC, we applied lentivirus-mediated gene silencing to mouse aortic ring assays. The lentivirus transduction efficiency on aortic ring was evaluated with GFP expression by fluorescence

microscopy and cytofluorimetry. About 50% of aortic ring cells were GFP positive when infected with more than 1×10^6 viral particles (Fig. S5A), and most of the vascular outgrowths were GFP positive, showing that sprouting EC were efficiently infected with lentiviral vectors (Fig. S5B). By applying this method we were able to silence $\alpha 6$ integrin expression in aorta and angiogenic sprouts, which are both positive for $\alpha 6$ integrin immunostaining (Fig. S6A,B). A reduction of mItg $\alpha 6$ expression, evaluated by real-time PCR on cells extracted from the gel, was observed in aortic ring infected with two different shRNA, shITGA6_48 and shITGA6_50 (Fig. S6C). Aortic rings infected with the scrambled shRNA, after embedding in BME matrix and VEGF-A/FGF-2 stimulation, sprouted forming tubular structures (Fig. 4A). In contrast aortic rings silenced for Itg $\alpha 6$ displayed reduced ability to make capillary-like structures: both shITGA6_48 and shITGA6_50 significantly inhibited sprout formation at day 4 and 6 after BME embedding (Fig. 4A). Blockade of integrin by addition of anti- $\alpha 6$ antibody to BME gel, resulted in similar levels of sprouting inhibition (Fig. S7A). In accordance with our own in vitro observations, $\alpha 6$ integrin down-regulation did not inhibit or delay the formation of capillary-like structures from aortic rings embedded in type-I collagen gel (Fig. 4B). These results confirmed that $\alpha 6$ integrin was functionally involved in the process of endothelial sprouting in a ligand-dependent manner.

BM components control endothelial podosomes formation in a concentration-dependent manner

Since we have observed the role of interaction $\alpha 6$ integrin-laminin in angiogenesis, we decided to analyze one of the types of adhesions important in invasion of tissue boundary: podosomes, i.e. specialized plasma-membrane microdomains that combine adhesive and proteolytic activities to spatially restricted sites of matrix degradation. It is known that in endothelium the phenomenon of podosomes formation is related to BM degradation [36], but the role of the principal components of

BM – laminin and type-IV collagen – in the control of podosome assembly has not yet been addressed.

Therefore, we seeded EC on type-I collagen film by adding different concentration of laminin or type-IV collagen before gel solidification. EC were treated with phorbol ester (PMA) for 1 hour, and podosome formation was measured after immunostaining of F-actin and cortactin, most important markers of podosomes, as described in the literature [37]. Upon stimulation of PMA, stress fibers rapidly disappeared and F-actin dots and rings became detectable. Podosomes remained visible up to 3 hours and then progressively disappeared [38].

Curiously, the presence of laminin and type-IV collagen in the matrix film induces different EC behaviors in a concentration-dependent manner: growing concentration of laminin decreases the percentage of podosome positive cells (a decrease of 2% per doubling of laminin), while type-IV collagen increases podosome formation in EC (an increase of 2% per halving of laminin) (Fig. 5A). Similar results were obtained on 1% gelatin film with addition of laminin, by confirming that this biological behavior is linked solely to laminin concentration and not to type-I collagen interaction with EC (Fig. 5B). Moreover, we asked us whether the gelatin film on coverslips has some amount of laminin and, by using a curve of immunofluorescence intensity of laminin on coated coverslips, we have seen that 1% porcine gelatin has a mean laminin concentration of about 2 $\mu\text{g/ml}$ (Fig S8A-B).

It is known that Src regulates podosome assembly in cultured endothelial cells in response to PMA [38] and also that, in podosome formation upon growth factor stimulation, activation of Rac1 leads to cortactin re-localization from internal cytoplasmic regions to the cortical actin network [39-41]. Therefore, Src and cortactin local amounts in podosomes can be considered the indicators of maturation of podosomes. To analyze whether laminin changes the maturation and assembly of endothelial podosome, we investigated the amount of Src and cortactin in podosome ROI in

condition with laminin concentrations. We observed with confocal microscopy visualization and quantification that the presence of laminin reduces the maturation of podosome by decreasing Src and cortactin fluorescence in podosome ROI in a concentration-dependent manner (Fig 5C-D), by not modulating the mean diameter of podosomal actin-cortactin ring (Fig. S9A). In contrast, podosomal cortactin localization is not modulated in EC seeded on growing concentration of type-IV collagen (Fig. S9B).

These results suggest that laminin decreases capability of endothelial podosome formation, by decreasing the assembling maturation of podosome in terms of Src and cortactin amounts in podosomes.

Integrin $\alpha 6$ is recruited in endothelial podosomes

Since laminin changes the maturation of podosome assembly, by reducing the amount of Src and cortactin in podosome, we hypothesized that integrin $\alpha 6$ or $\alpha 3$ – the only two possible laminin-binding α -integrins in human cultured EC – was functionally recruited in podosome.

Therefore, to test whether integrin $\alpha 6$ colocalized with podosomes, we stained EC with antibodies against integrin $\alpha 6$, cortactin and F-actin. Integrin $\alpha 6$ staining is localized in the ring of podosome (Fig. 6A), as already demonstrated for other integrin complexes, ie $\alpha v \beta 3$ [38]. On the contrary, immunofluorescence analysis on PMA-stimulated EC unveils that integrin $\alpha 3$ is not recruited in podosome structures, as shown in Figures S10A where it is evident the non-colocalization of integrin $\alpha 3$ with actin-cortactin ring.

Moreover, after PMA stimulation $\alpha 6$ integrin is re-localized from focal adhesions and perinuclear region to podosomes, by suggesting an active translocation of integrin $\alpha 6$ from pre-existing cellular adhesion compartment (Fig S11A-B). In fact, it is known that, unlike focal

adhesions, podosome assembly does not require *de novo* protein synthesis [42] and podosome formation therefore proceeds much faster (1 h versus 3 h).

As described above, although $\alpha 6$ can form both $\alpha 6\beta 1$ and $\alpha 6\beta 4$ heterodimers, human cultured EC do not express detectable levels of integrin $\beta 4$, therefore it is presumable that only the $\alpha 6\beta 1$ heterodimer was present in podosome zone (data not shown and [17]). $\beta 1$ integrin has been already described to be in endothelial podosomes [43], but its specific function has not yet been addressed.

To analyze the precise localization of integrin $\alpha 6$ in the structure of podosome, we collected high-resolution confocal image stacks of EC stained with anti-cortactin, anti- $\alpha 6$ integrin antibody and phalloidin to reconstruct 3D volume rendering of podosome. As shown in Figure 6B, integrin $\alpha 6$ staining forms, in common with cortactin-actin staining, the classical podosome ring-like structure. Moreover, it is noticeable that integrin $\alpha 6$ is localized in the zone nearer to ECM and in the zone surrounding the core of the cortactin-actin ring.

We further investigated whether these structures indeed constitute adhesions by using TIRF (total internal reflection fluorescence) microscopy. The zones of close adhesion (<90 nm distance) to the substratum of cortactin and integrin $\alpha 6$ in EC were stained by immunofluorescence and visualized by TIRF signal (Fig. S10B). Colocalization of both TIRF signals revealed that most probably integrin $\alpha 6$ is actively implicated in close adhesion to laminin of the substratum in podosome zones.

Laminin controls podosome formation by decreasing integrin $\alpha 6$ localization to podosomes

Since we have seen an inverse proportion of podosome formation in response to laminin concentration, we asked ourselves how laminin inhibits podosome assembly. We investigated the quantities of integrin $\alpha 6$ and integrin $\alpha 3$ localized to podosome in response to laminin concentration

in gelatin film. Curiously, we observed with confocal microscopy quantification that laminin reduces recruitment of integrin $\alpha 6$ in podosome. The addition of laminin - 5, 10 or 20 $\mu\text{g/ml}$ in gelatin film - decreases of about 50% of integrin $\alpha 6$ staining in podosome ROI. On the contrary, as expected, integrin $\alpha 3$ – the other possible candidate for laminin-dependent effect on podosome – is not modulated by different laminin concentrations (Fig. 6C).

To examine whether $\alpha 6$ integrin controls podosome formation, we inhibited integrin function by gene silencing. Integrin $\alpha 6$ stable silencing and control shScr1 did not alter cell viability and cell morphology (data not shown). EC, seeded on gelatin film, were treated with PMA, and podosome formation was measured. As shown in Figures 6D, EC silenced with either shITGA6_4 or shITGA6_5 decreased the podosome formation by about 30% in comparison with shScr1 EC. Functional blockade of integrin by the addition of anti- $\alpha 6$ antibody in the moment of EC seeding resulted in similar levels of podosome formation inhibition (Fig. 6E), although in these conditions anti- $\alpha 6$ treatment did not inhibit 2-hours adhesion capability of EC (data not shown).

Our data suggest that laminin blocks endothelial podosome formation, by decreasing integrin $\alpha 6$ localization in podosome.

***In vivo* down-regulation of integrin $\alpha 6$ affects podosomes formation in EC layer**

In order to exclude that laminin and levels of $\alpha 6$ integrin solely affect the podosome formation of cultured EC, we investigated *in vivo* podosome formation in the native endothelium in response to TGF β , VEGF-A or PMA. We used a previously described *in vivo* model to analyze the formation of podosomes in aortic vessels, Rottiers *et al.* demonstrated that upon TGF β stimulation EC of aortic vessels present podosome rosettes that degrades specifically type-IV collagen and not laminin in arterial BM [36]. We showed that endothelial podosomes were induced also upon VEGF-A and

PMA stimulation in aortic vessels (Fig. 7A) and that the features of VEGF and PMA-induced podosomes are similar to those described by Rottiers *et al.* – with a mean diameter of $8,1\pm 0,4$ μm and marked by cortactin, vinculin, F-actin and FAK (data not shown). This model showed a high efficacy to analyze whether integrin $\alpha 6$ and consequently laminin have a crucial role in native endothelium podosome formation.

Therefore, we analyzed whether also in native endothelium integrin $\alpha 6$ colocalized with endothelial rosettes upon TGF β , VEGF-A or PMA stimulation. As showed in Figure 7B, integrin $\alpha 6$ staining is localized in the ring of podosome, as already demonstrated above *in vitro* EC, and this localization was demonstrated with TGF β , VEGF-A or PMA stimulation (data not shown).

However, by a high-resolution confocal magnification, integrin $\alpha 6$ was showed in the borders of ring structure that surrounds the podosome core – region typically described for integrin adhesion [2] – while cortactin and F-actin staining marks precisely the ring of podosome (Fig. 7C).

By applying the lentiviral transduction of shRNA, described above, we were able to silence $\alpha 6$ integrin expression in aorta in order to investigate indirectly also the role of laminin in *in vivo* formation of podosomes. As shown in Figures 7D, upon TGF β aortic segments silenced with either shITGA6_48 or shITGA6_50 failed to form podosomes, detected by cortactin-actin staining. The reduction of podosome formation was by about 30% in comparison with shScr1 infected aortic vessels.

Our results demonstrate that laminin and – consequently – $\alpha 6$ integrin, over to guide podosome formation *in vitro*, impairs *in vivo* podosome formation in aortic vessels.

BM directs migration of tip cells by localizing the activation of VEGF pathway in EC

As a final point, since ECM degradation and tip cells migration are directed towards BM in sprouting angiogenesis process, we investigated how BM establishes polarization of EC in aortic vessels. To study and visualize the morphology and geometry of tip cells sprouting in response to composition of ECM, we designed a 3D sprouting model, called Mouse Aortic Sheet, by using explanted murine aortas cut along their long axis and embedded in ECM gel. This model showed a high efficacy to visualize sprouting angiogenesis in condition to different compositions of ECM.

We decided to analyze the sprouting angiogenesis in condition to ECM: components of interstitial ECM, such as type-I collagen gel, and vBM components, such as BME. Interestingly, into type-I collagen gel VEGF-driven angiogenic outgrowths sprouted only along the four borders of the aortic explants and never from the apical side of endothelial layer (Fig. 8A). On the contrary, when EC apical side was exposed to BME components, sprouting angiogenesis involved also the center of EC layer. In Figure 8B it is shown a magnification of section view of a sprouting EC in the center of apical side of aortic segment endothelium. This event only happened when Aortic Sheets were embedded in BME or in type-I collagen gel plus BME components (data not shown).

To explain our results with mouse Aortic Sheets sprouting, we hypothesized that physiologically VEGFR2 was phosphorylated only in basal zone, where EC have contacts with vascular BM. When we expose EC apical side to BM contact, EC is involved in a re-polarization of VEGFR2 localization and consequently phosphorylation.

Therefore, to test this hypothesis, we analyzed the localization of phospho-VEGFR2 in EC of Aortic Sheets covered by a thin layer of ECM gel and stimulated for 24 hours with 30 $\mu\text{g/ml}$ VEGF-A. Interestingly, as showed in Figure 8C, only some EC were stained with p-VEGFR2 immunofluorescence – probably the future putative tip cells. Moreover, the localization of staining is

higher in basal side of EC within Aortic Sheets covered by type-I collagen gel (Fig. 8D), while EC layer in Aortic Sheet covered by BM extract gel showed a more homogeneous activation of VEGFR2 (Fig. 8E).

To summarize our data and hypothesis about the cause of differential sprouting angiogenesis patterns of Aortic Sheets into ECM gel, we show the schematization of polarization of EC layer covered by type-I collagen or BM extract gel (Fig. 8F-G).

Finally, to understand how and which BM components drives the localized phosphorylation of VEGFR2, we analyzed the localization of phospho-VEGFR2 in cultured EC seeded on gelatin with addition of growing concentration of laminin or type-IV collagen. We have studied the phosphorylation of VEGFR2 in apical and basal side of EC, by analyzing their z-section (Fig. 9A). After 5 minutes of VEGF stimulation EC on gelatin showed a ratio apical:basal p-VEGFR2 fluorescence similar to 1, but this ratio decreased in condition to amount of laminin in substrate in a concentration-dependent manner (Fig. 9B): with growing concentration of laminin the activation of VEGFR2 is higher in basal side and lower in apical one of EC. Since the principal ligand of laminin in EC is integrin $\alpha 6$, we examined also the localization of integrin $\alpha 6$ in EC seeded on growing concentration of laminin. As expected, fluorescence of staining for integrin $\alpha 6$ increased in basal side in condition to concentration of laminin in substrate, but, surprisingly, the trend of apical:basal ratio is very similar to that of p-VEGFR2 (Fig. 9B), by suggesting an interaction of integrin $\alpha 6$ with VEGFR2. In contrast, the addition of type-IV collagen in the substrate does not significantly modify the apical:basal ratio of p-VEGFR2 and integrin $\alpha 6$ staining (Fig. 9C).

Taken together, our data suggest that BM, and more precisely laminin, guides sprouting angiogenesis, by modulating EC polarization, in which is crucial a localized activation of VEGFR2 and the distribution of integrin $\alpha 6$ and in the zone adjacent to BM, both events that could define the leading edge of tip cell and consequently of the angiogenic sprouting.

DISCUSSION

Integrin $\alpha 6$, receptor for laminin, modulates sprouting angiogenesis

Tumor cells, macrophages, and fibroblasts within tumors or within physiological conditions could secrete factors such as VEGF-A and FGF-2, which induces sprouting angiogenesis and blood vessel growth [44]. These growth factors activate or up-regulate the expression of vascular integrins such as $\alpha 1\beta 1$, $\alpha 2\beta 1$, $\alpha 4\beta 1$, $\alpha 5\beta 1$, and $\alpha v\beta 3$ [45], which in turn promote EC migration and survival during sprouting angiogenesis. Although integrins binding to provisional ECM have been extensively studied, the role of integrins that bind components of vascular BM such as laminins is less clear. In fact, laminin-binding integrins such as $\alpha 6\beta 1$ and $\alpha 3\beta 1$ are considered important for the process of endothelial tube stabilization, and their role in regulating sprouting angiogenesis is uncertain [46]. Here, we show that $\alpha 6$ integrin is up-regulated by angiogenic factors in EC. Although it is known that $\alpha 6$ integrin is expressed in human and mice endothelium, there has been no evidence thus far of its up-regulation during angiogenesis [17].

EC in which $\alpha 6$ integrin is down-regulated defects in the ability to migrate and form tubular structures on laminin-containing matrix are prominently displayed. However, when similar experiments were performed on ECM ligands other than laminin, the $\alpha 6$ integrin down-regulation did not modify the EC response. It is known that the effects of ECM on vascular cell walls differs greatly, depending on the state of the vessel and, to a lesser extent, on the vessel type. For these reasons, the role of $\alpha 6$ integrin has been studied in the aortic ring model. By setting up the

knockdown of $\alpha 6$ integrin in aortic rings using a lentiviral vector strategy, we further showed that endothelial $\alpha 6$ was required for sprouting from the aortic ring toward BME, but not type I collagen. It is evident that switching from quiescent endothelium to an angiogenic endothelium implies marked changes in ECM interactions in which EC are involved. Interestingly, the ECM features change along the angiogenic process from an established laminin and collagen IV-enriched to a provisional matrix, mainly constituted by collagen I, vitronectin, and fibronectin [4]. It is likely that modulation of $\alpha 6$ integrin levels could play a role in this switch. The high levels of $\alpha 6$ integrin could allow EC to invade BM, probably counteracting the effect of “stabilizing” integrins, whereas invading EC, which interact with collagen, are not dependent on this integrin. Therefore, we propose that $\alpha 6$ integrin is required only in the early phases of EC sprouting from a mature vessel.

Laminin, through integrin $\alpha 6$ binding, blocks endothelial podosome formation and consequently BM degradation

In order to investigate the implication of integrin $\alpha 6$ in EC invasion of BM, we studied the formation of endothelial podosome, specialized plasma-membrane microdomains that combine adhesive and proteolytic activities to spatially restricted sites of matrix degradation.

Therefore, we decided to analyze the role of laminin and integrin $\alpha 6$ in the formation of endothelial podosome. Here, we demonstrate that growing concentrations of laminin block podosome formation in EC, by decreasing the localization of cortactin, src and integrin $\alpha 6$ in the podosome. By applying gene silencing of $\alpha 6$ integrin in EC in culture and in *in vivo* aortic vessels using a lentiviral vector strategy, we further show that endothelial $\alpha 6$ is required for podosome formation.

In physiological conditions, podosomes form spontaneously in certain cells such as macrophages and immature dendritic cells, which share the common feature of travelling across tissue boundaries

[2, 23, 37]. Although recently it has been demonstrated the presence of podosome rosettes in the native endothelium [36], the pathophysiological function of endothelial podosome is unclear. Our results about $\alpha 6$ integrin and podosome in condition to vBM components suggest a decisive implication of podosome in invasion of BM in the early stages of sprouting angiogenesis.

We propose that the presence of high concentration of laminin in BM could stabilize EC in a quiescent and podosome-negative phenotype – with low $\alpha 6$ integrin levels – and, only when $\alpha 6$ integrin expression is up-regulated by VEGF-A persistent stimuli (48 hours), EC could form podosomes, degradate matrix and invade BM, by starting tip cell sprouting angiogenesis. Moreover, it was demonstrated that in early stages EC degradate only type-IV collagen and not laminin [36], this detail could suggest that EC uses the binding $\alpha 6$ integrin-laminin as hold in the process of BM invasion.

Laminin directs the leading edge of sprouting angiogenesis

Few is known about the very early stages of sprouting angiogenesis and about how tip cell could cross the barrier of BM. Therefore, our last question was whether BM could influence the tip cell sprouting and how it could happen.

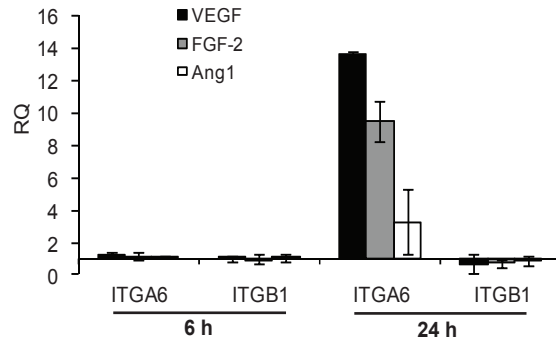
It is well-known that VEGF-A is the most important chemoattractant for EC and sprouting [1, 3, 29, 44] and that VEGF-A guides angiogenic sprouting utilizing endothelial tip cell filopodia [47]. Moreover, recently Jakobsson *et al.* have described the process of dynamical competition for tip cell position through relative levels of VEGFR2 [48]. Although the role of VEGF-A and VEGFR2 in sprouting angiogenesis guiding have been extensively studied, the role of vascular BM – the first real barrier of tip cell – in VEGFR2 activation of quiescent-angiogenic endothelium is less clear.

In this work, we demonstrate that vascular BM, and more precisely laminin, influences the activation of VEGFR2 and the localization of integrin $\alpha 6$ *in vivo* and *in vitro* EC. The presence of vascular BM components controls the distribution of sprouts in Aortic Sheets, by allowing angiogenic outgrowth also in the center of EC layer. In according to our data, tip cell could start sprouting angiogenesis by solely invading BM, because the activation of VEGFR2 is confined only in the basal side of EC layer. And so, when we cultured Aortic Sheets in BME, we would “deceive” EC, by causing the re-polarization of EC layer, because EC feel BM components and VEGF-A stimulus in the apical side. This influence could be applied by integrin $\alpha 6$, that localizes in basal side of EC in condition to laminin addition.

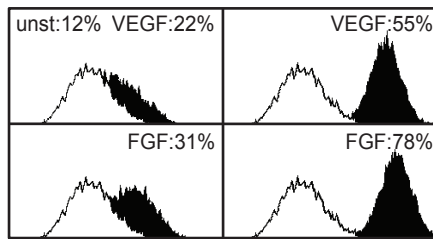
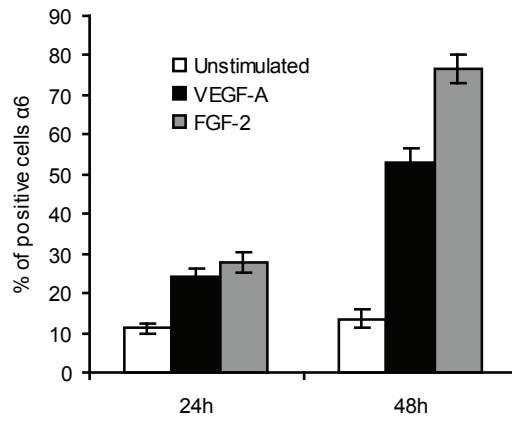
Therefore, our initial data about integrin $\alpha 6$ role in sprouting angiogenesis could be explained by $\alpha 6$ implication in formation of endothelial podosomes and by its role in polarization of EC; both of these functions seem crucial in invasion of BM, step of sprouting angiogenesis yet to elucidate precisely.

Fig.1

A



B



C

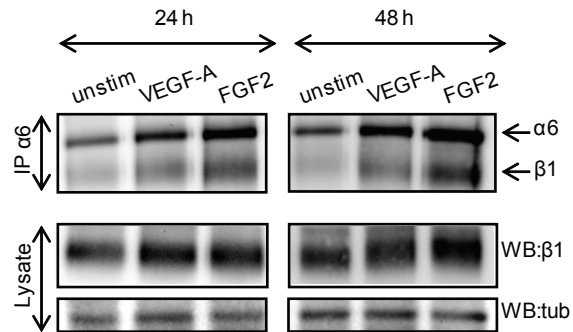


Fig.2

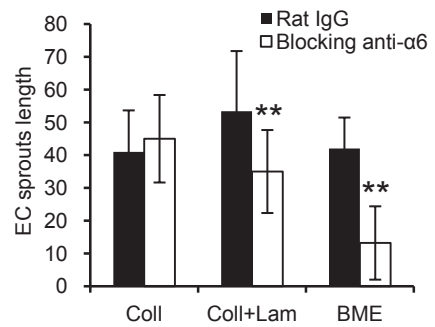
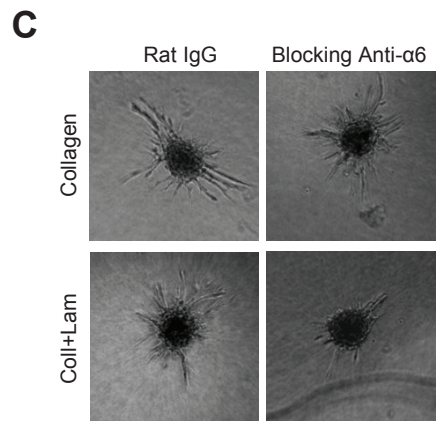
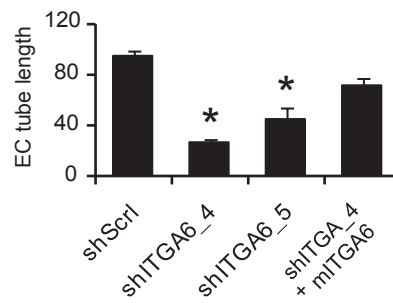
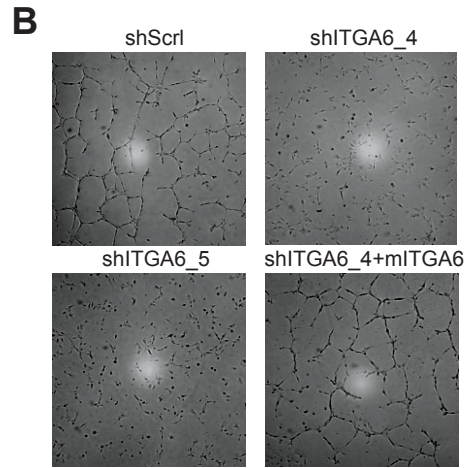
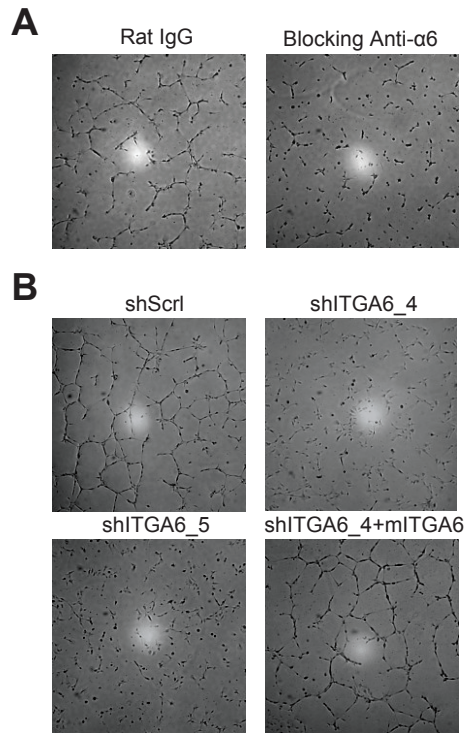
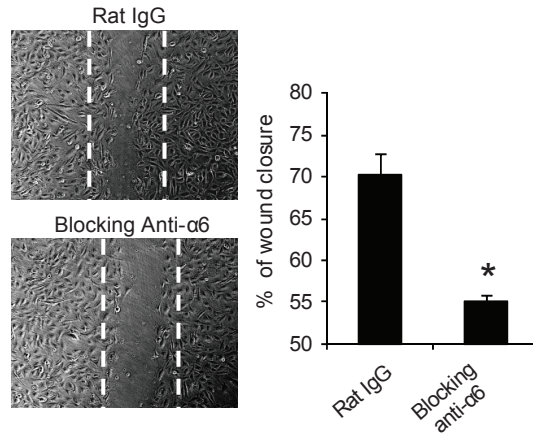
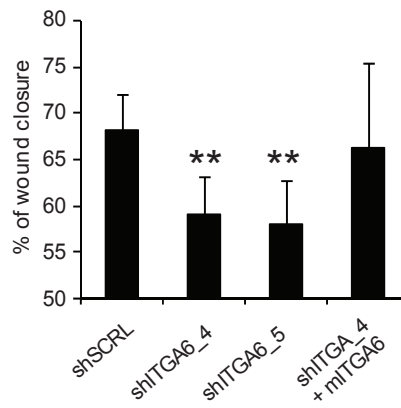


Fig.3

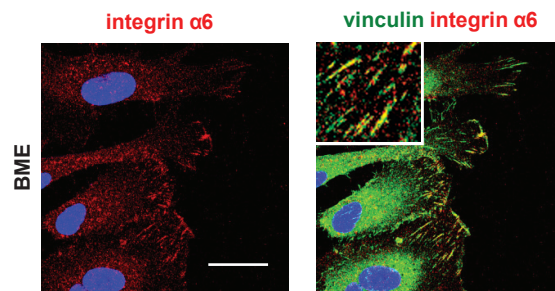
A



B



C



D

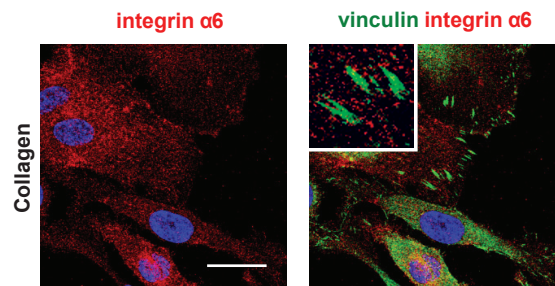
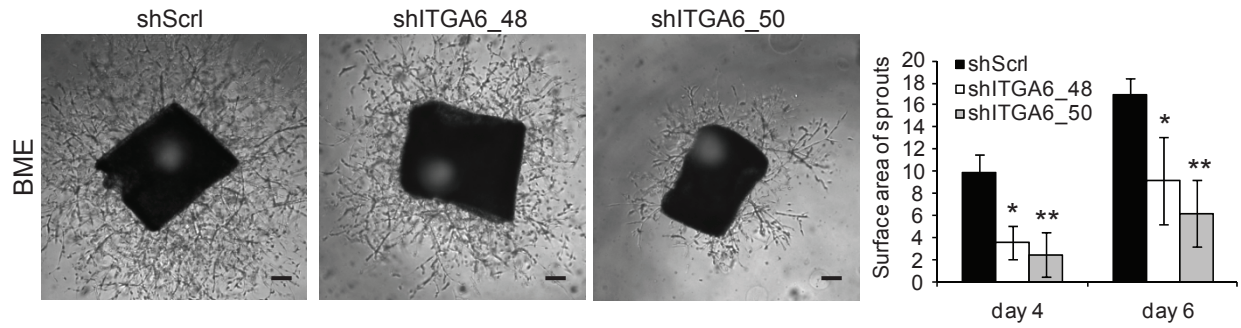


Fig.4

A



B

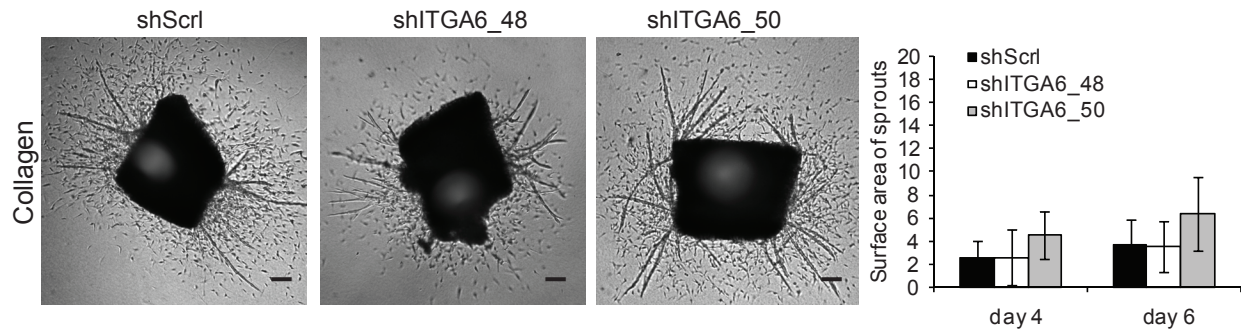
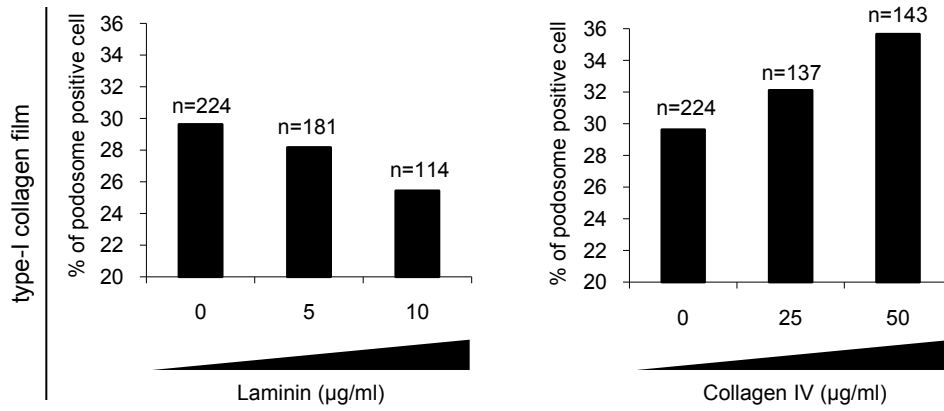
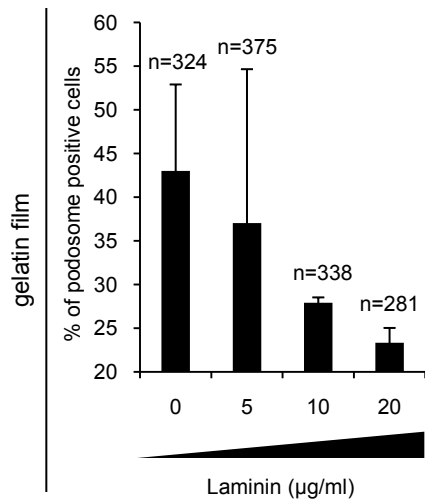


Fig. 5

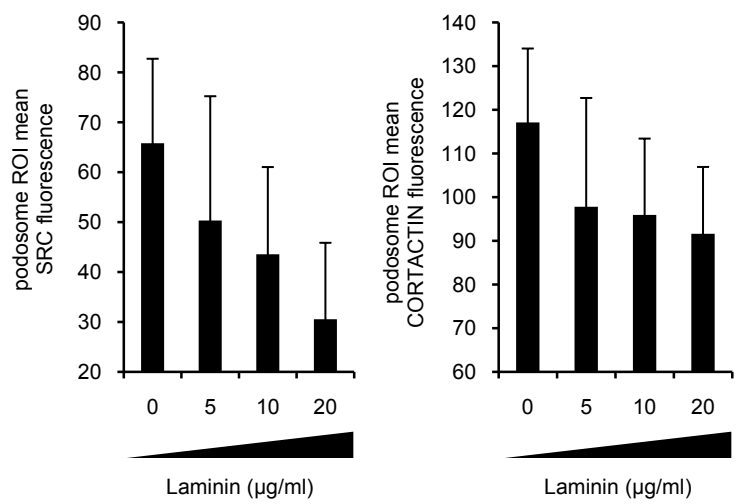
A



B



C



D

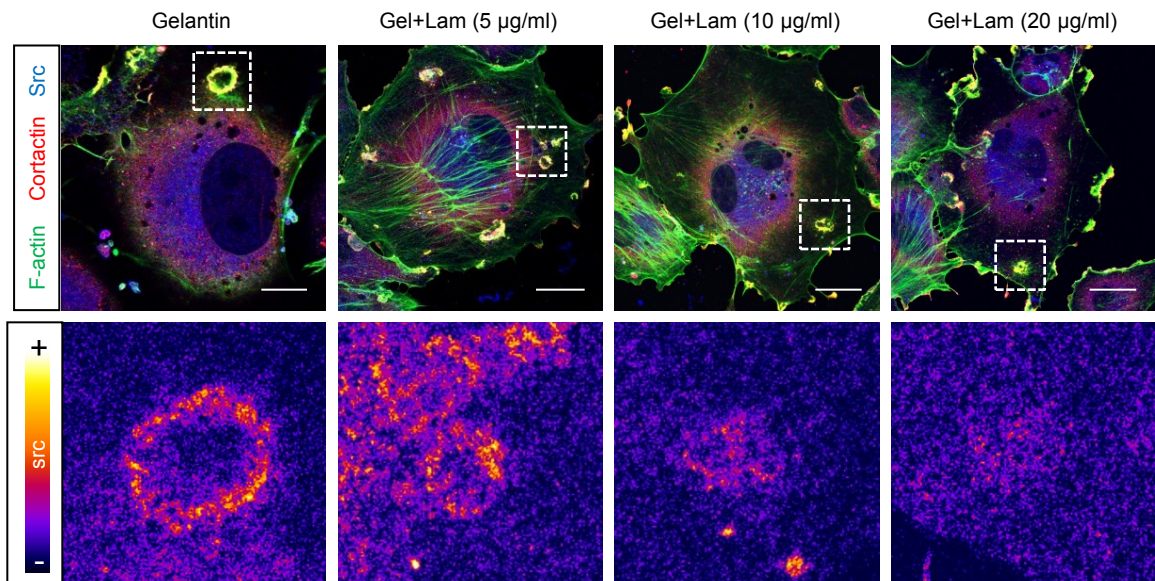
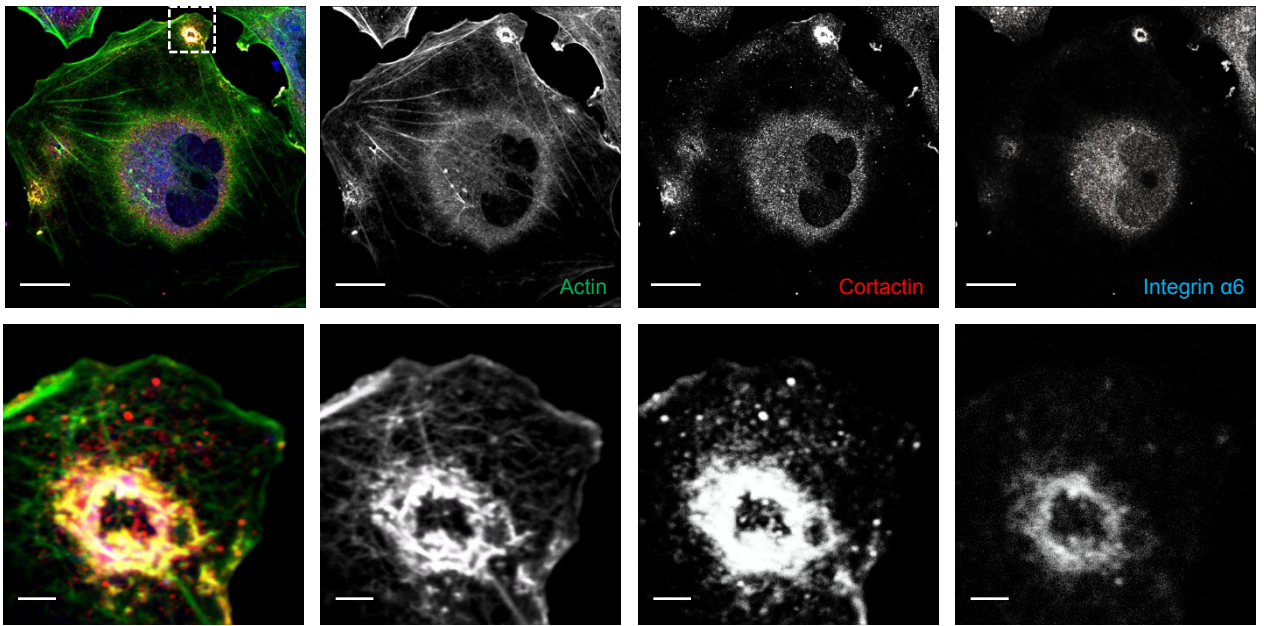
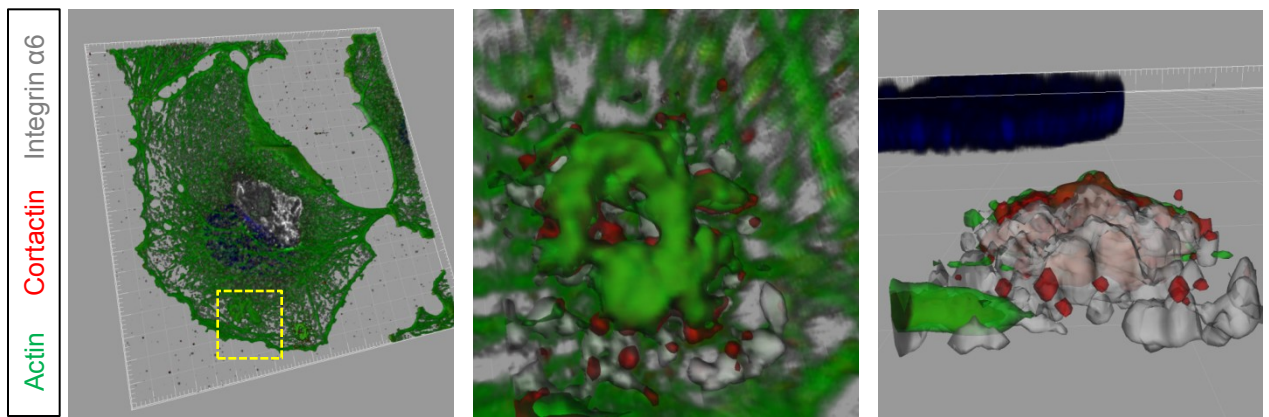


Fig. 6

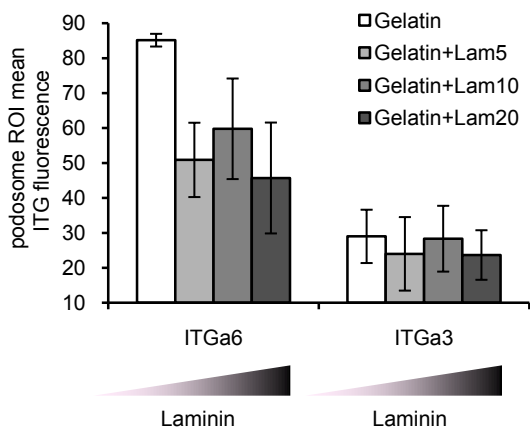
A



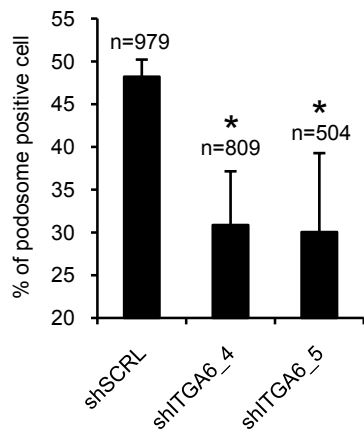
B



C



D



E

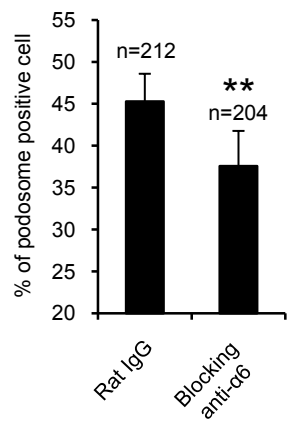
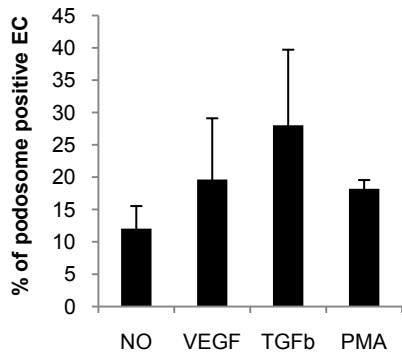
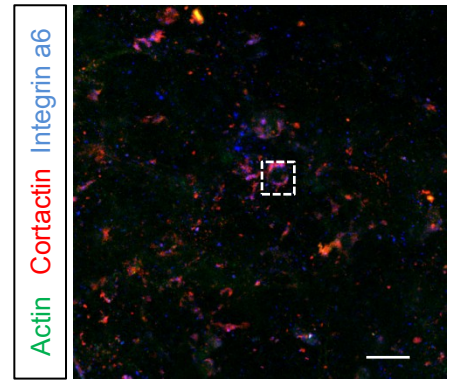


Fig. 7

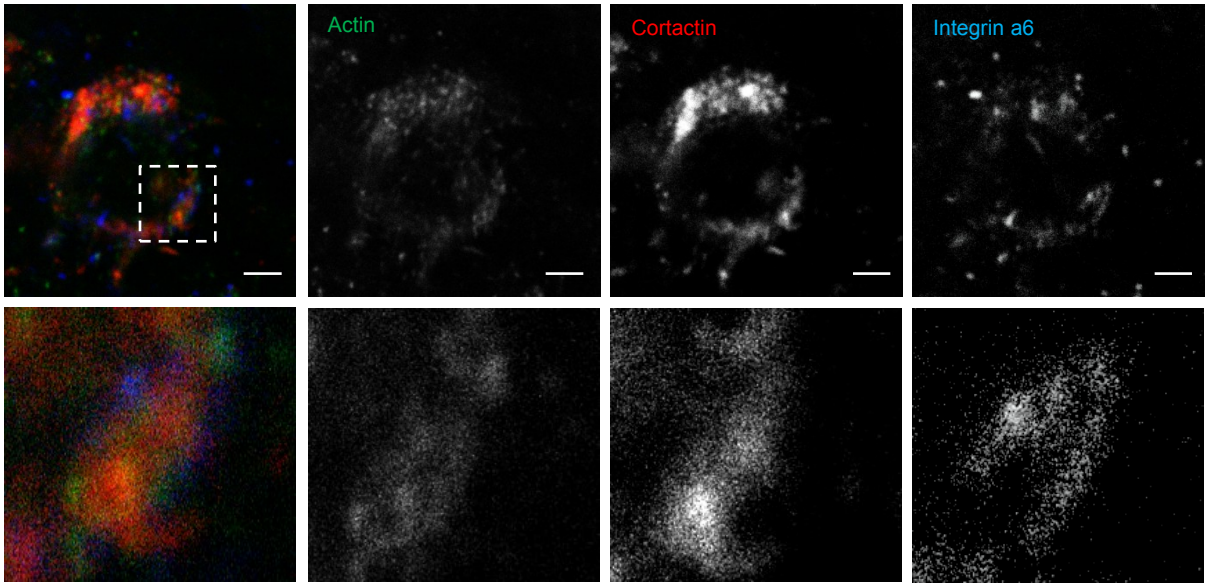
A



B



C



D

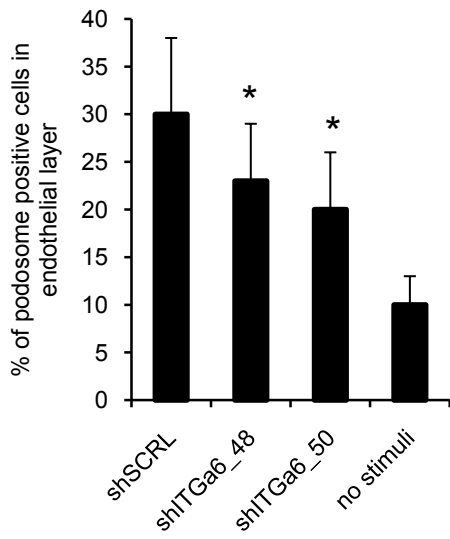


Fig. 8

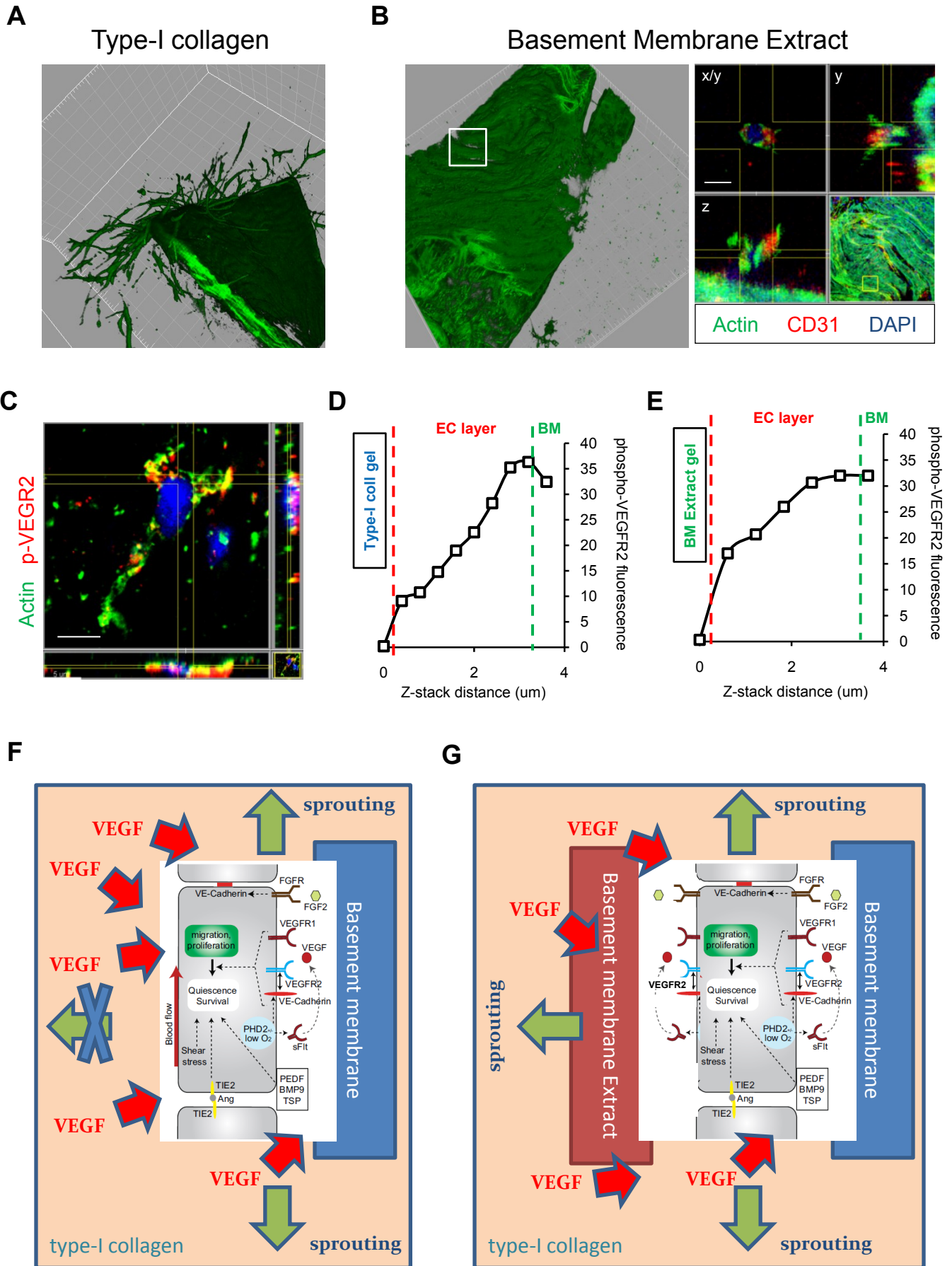
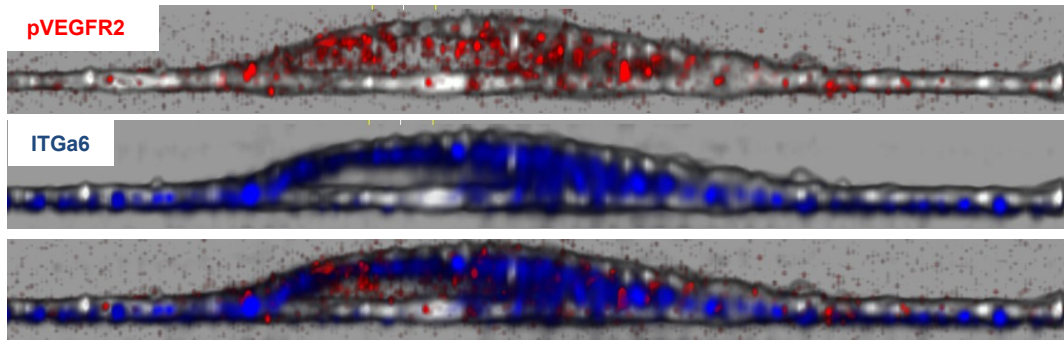
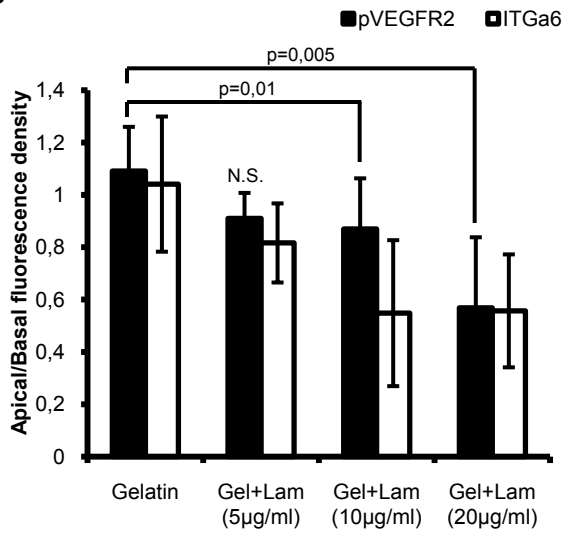


Fig. 9

A



B



C

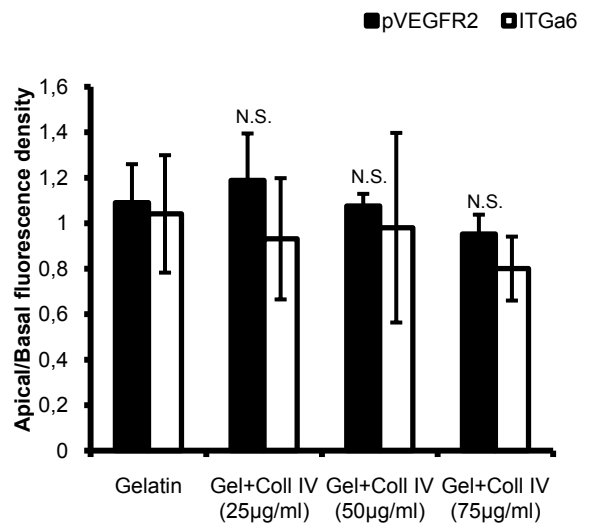


FIGURE LEGENDS

Figure 1. Modulation of $\alpha 6$ integrin expression by angiogenic growth factors. (A) qRT-PCR on mRNA from EC treated for 6h or 24h with VEGF-A, FGF2 or Angiopoietin-1. Relative quantification (RQ) of $\alpha 6$ and $\beta 1$ integrin mRNA levels are calculated on mRNA levels normalized to GAPDH and compared with unstimulated EC. (B) Cytofluorimetric analysis of $\alpha 6\beta 1$ integrin membrane expression on EC treated with VEGF-A or FGF-2. Graph shows the percentage (%) of EC expressing $\alpha 6\beta 1$ integrin, treated as indicated, in 3 independent experiments, each in triplicate (* $P < 0.01$ versus unstimulated). (C) EC treated as indicated were biotinylated and lysed. $\alpha 6$ integrin was immunoprecipitated, subjected to Western blotting followed by detection with streptavidin. The same lysates were analyzed using anti- $\beta 1$ antibody and anti-tubulin.

Figure 2. $\alpha 6$ integrin is required for endothelial cells tubulogenesis on basement membrane but not in collagen gel. (A) EC, transduced with control shRNA (ShScr1), ITGA6 specific shRNAs (shITGA6_4, shITGA6_5) and ITGA6 specific shRNA with mouse ITGA6 cDNA (shITGA6_4+mItga6), were seeded on BME gel and photographed after 8h. Quantification of capillary-like network length was performed with WinRhizo imaging software. Values shown are average \pm SD of 3 independent experiments, each in triplicate. (* $P < 0.01$ versus shScr1) (B) EC seeded on BME gel, treated with rat IgG and anti- $\alpha 6$ blocking antibody respectively, and photographed after 8h. Photographs are representative of three experiments. (C) Spheroids of EC, transduced as indicated above, were embedded in collagen gel in the absence or presence of VEGF-

A and FGF-2, and observed after 48h. Photographs are representative of 3 different experiments with more than 10 spheroids each.

Figure 3. Motility on basement membrane extract is affected by $\alpha 6$ integrin down-regulation. (A) EC, treated with rat IgG and anti- $\alpha 6$ blocking antibody, or transduced as indicated (B), were plated on plastic coated with BME and induced to migrate across an artificial wound in response to VEGF-A and FGF2. White broken lines delimitate the initial positions of wounds. Graphs show mean percentage of wound closure after 7h of migration \pm SD of 3 independent experiments, each in triplicate. (* $P < 0.01$ versus rat IgG; ** $P < 0.05$ versus shScrl). (C-D) EC migrating across an artificial wound were fixed and stained with anti-integrin $\alpha 6$ (red), anti-vinculin (green) and DAPI (blue). EC were plated on BME (C) or type I collagen (D) coated coverslip. Insets are high magnification of the same photograph. Scale bar: 50 μ m.

Figure 4. $\alpha 6$ integrin promotes sprouting angiogenesis into basement membrane extract gel in mouse aortic rings. Aortic rings were transduced with lentiviruses carrying scramble shRNA (shScrl) and shRNA targeting ITGA6 (shITGA6_48 and shITGA6_50), and observed after 6 days in BME (A) and collagen gel (B). Photographs are representatives of three experiments (scale bar: 100 μ m). Sprouting angiogenesis was quantified 4 and 6-days after matrix gel embedding, as tubular areas. Values are means \pm SD of three independent experiments, each in quintuplicate and from different mice (* $P < 0.05$ versus shScrl; ** $P < 0.01$).

Figure 5. Laminin inhibits podosome formation and maturation in cultured EC. (A) EC were seeded on type-I collagen film with addition of laminin or type-IV collagen with the final concentration written in x -axis. (B) EC were seeded on gelatin film with addition of laminin with the

final concentration written in *x*-axis. Quantification of cells containing podosomes, stimulated with PMA and detected by immunostaining of F-actin and cortactin. Data are presented as percentage of the total population. Error bars represent the mean \pm SD of total *n* cells from three independent experiments. (C) Quantification of src and cortactin in podosome ROIs of EC in experiment described in B. Columns, mean fluorescence detected in podosomes ROI, identified with F-actin-cortactin colocalization, of three independent experiments, six cells per experimental point each experiment; bar, SD. (D) High-resolution confocal image of representative EC, stained with phalloidin (green), anti-cortactin (red) and anti-src (blue), of experiment in B-C (bar, 20 μ m). The square dotted line (top) is enlarged in the bottom. For src fluorescence in the bottom has been used a look-up table (LUT) that color-codes images according to pixel intensity (blue=0; yellow=256).

Figure 6. Integrin α 6 is required for *in vitro* formation of podosome in EC. (A) Confocal images of a representative EC, stained with phalloidin (green), anti-cortactin (red) and anti-integrin α 6 (blue); (bar, 20 μ m). The square dotted line (top) is enlarged in the bottom (bar, 2 μ m). (B) High-resolution confocal image stack of EC podosome structure stained with phalloidin (red) anti-cortactin (green) and anti-integrin α 6 (gray) antibody were reconstructed by isosurface rendering using Imaris software. (C) Quantification of α 6 and α 3 integrin in podosome ROIs of EC seeded on gelatin film with addition of laminin with the final concentration written in legend. Columns, mean fluorescence detected in podosomes ROI, identified with F-actin-cortactin colocalization, of three independent experiments, six cells per experimental point each experiment; bar, SD. (D) EC, transduced with control shRNA (shScr1) and ITGA6 specific shRNAs (shITGA6_4, shITGA6_5), were seeded on gelatin film. (E) EC, treated with rat IgG or anti- α 6 blocking antibody, were seeded on gelatin film. Quantification of cells containing podosomes, stimulated with PMA and detected by immunostaining of F-actin and cortactin. Data are presented as percentage of the total population. Error bars represent

the mean \pm SD of total n cells from three independent experiments . (*P<0.05 versus ShScr1; *P<0.05 versus rat IgG).

Figure 7. Down-regulation of integrin $\alpha 6$ in aortic vessels affects *in vivo* endothelial podosome formation. (A) In vivo formation of podosomes in condition to different stimulation. Quantification of EC of aortic vessels containing podosomes, detected by immunostaining of F-actin and cortactin. Data are presented as percentage of the total cells in endothelial layer, calculated with DAPI normalization. Error bars represent the mean \pm SD of two aortic segments from three independent experiments. (B) Confocal image of endothelial layer of a representative aortic vessel, stained with phalloidin (green), anti-cortactin (red) and anti-integrin $\alpha 6$ (blue); (bar, 20 μm). The square dotted line (top) is enlarged in C (bar, 2 μm). (D) Aortic vessels, transduced with control shRNA (shScr1) and ITGA6 specific shRNAs (shITGA6_48, shITGA6_50), were stimulated with TGF β for 24 hours and analyzed with cortactin-actin staining. Data are presented as percentage of the total cells in endothelial layer, calculated with DAPI normalization. Error bars represent the mean \pm SD of two aortic segments from two independent experiments.

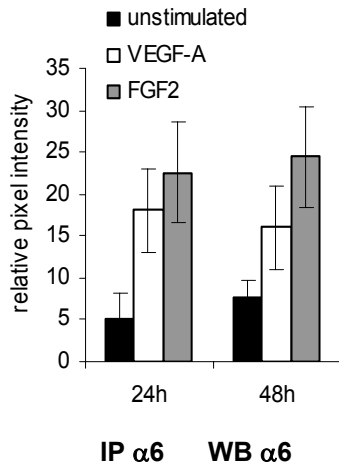
Figure 8. Vascular basement membrane guides sprouting angiogenesis in mouse aortic sheets. (A) Mouse Aortic Sheet Sprouting Assay in type-I collagen gel. High-resolution confocal image stacks of Mouse Aortic Sheet sprouts stained with phalloidin were reconstructed by 3D volume rendering using Imaris software. (B) Mouse Aortic Sheet Sprouting Assay in BME gel. High-resolution confocal image stacks of Mouse Aortic Sheet sprouts stained with phalloidin were reconstructed by 3D volume rendering using Imaris software. The square dotted line (top) is enlarged in right xyz -section panel (bar, 10 μm). (C) Confocal z -sections of a single representative EC of Aortic Sheets stimulated with VEGF for 24 hours (bar, 5 μm). (D-E) Z-profile quantification of

phospho-Y1175-VEGFR2 in EC layer of Aortic Sheets covered by type-I collagen (D) or BME gel (E) and stimulated with VEGF for 24 hours. (F-G) Schematic representations of EC polarization and consequently of sprouting angiogenesis in condition to BM components localization.

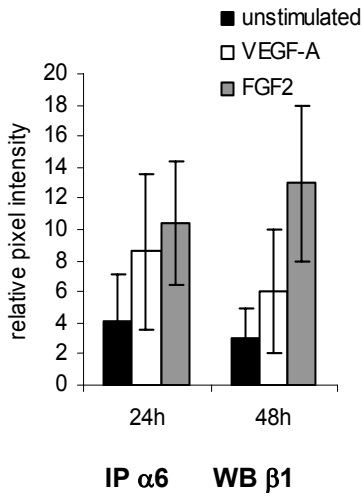
Figure 9. Laminin directs EC polarization thanks to activation of VEGFR2 and integrin $\alpha 6$ localization in basal side. (A) Representative 3- μ m-thick extended z-section of an EC seeded on gelatin. 3D volume rendering of EC stained with phalloidin (gray), anti-phospho-Y1175-VEGFR2 (red) and anti-integrin $\alpha 6$ (blue). (B) Quantification of apical:basal ratio of EC seeded on gelatin film with the addition of laminin with the final concentration written in *x*-axis. Measurement. Error bars represent the mean \pm SD of 10 EC from two independent experiments.

Supplemental Figure 1

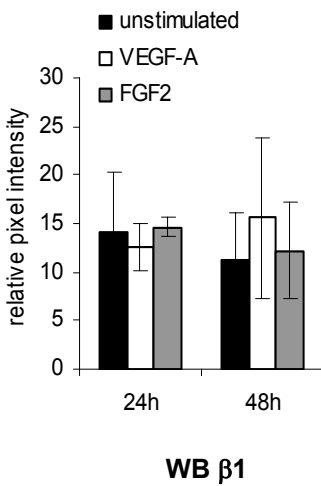
A



B

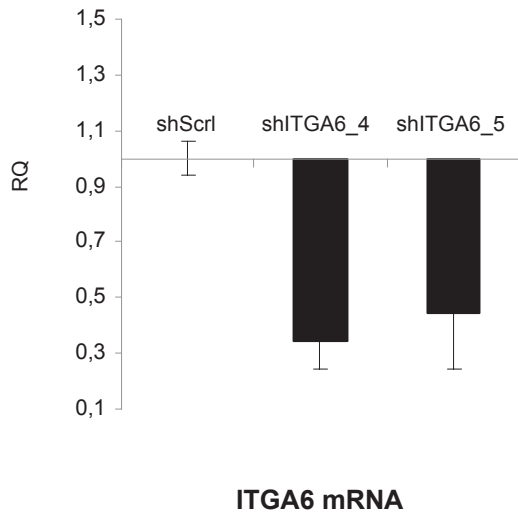


C

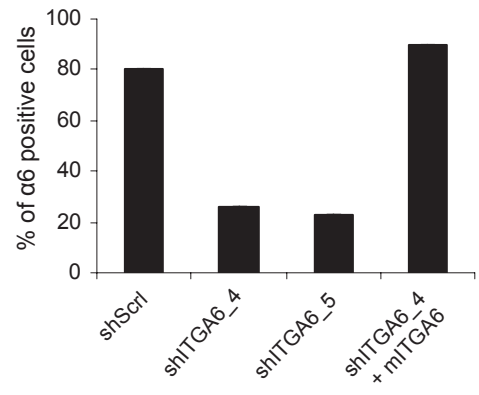


Supplemental Figure 2

A

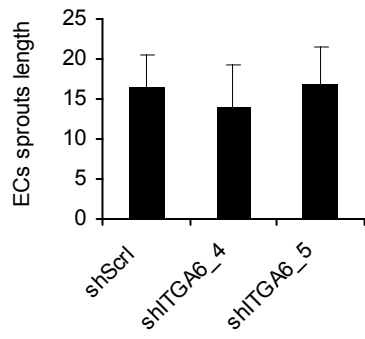
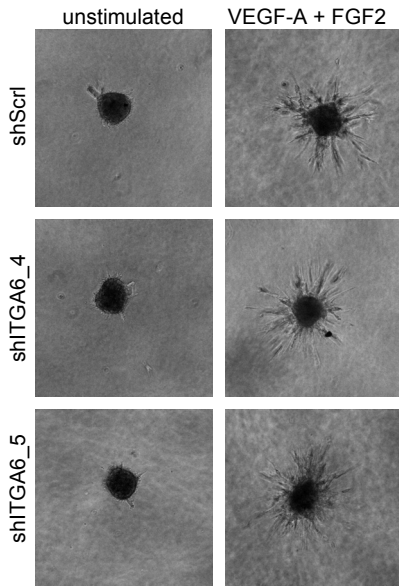


B

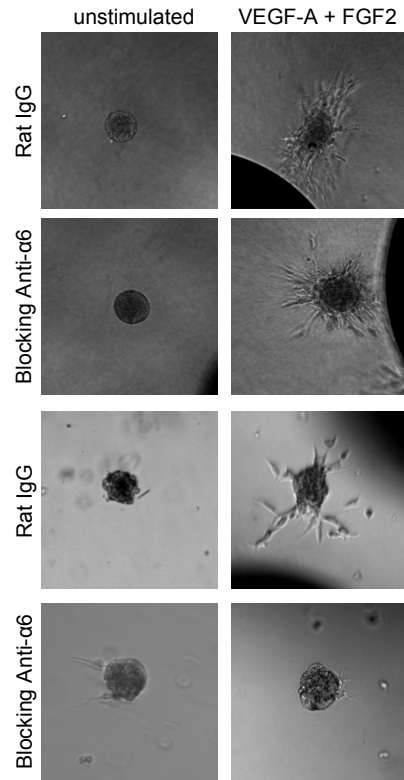


Supplemental Figure 3

A

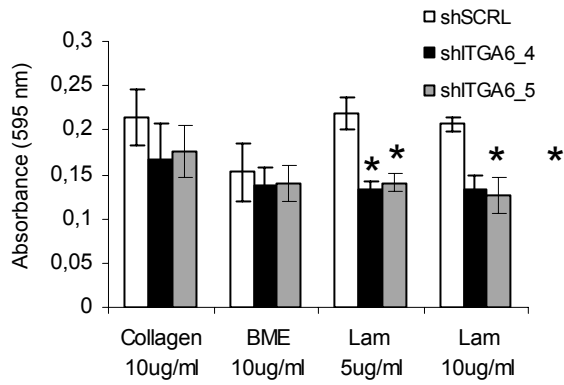


B

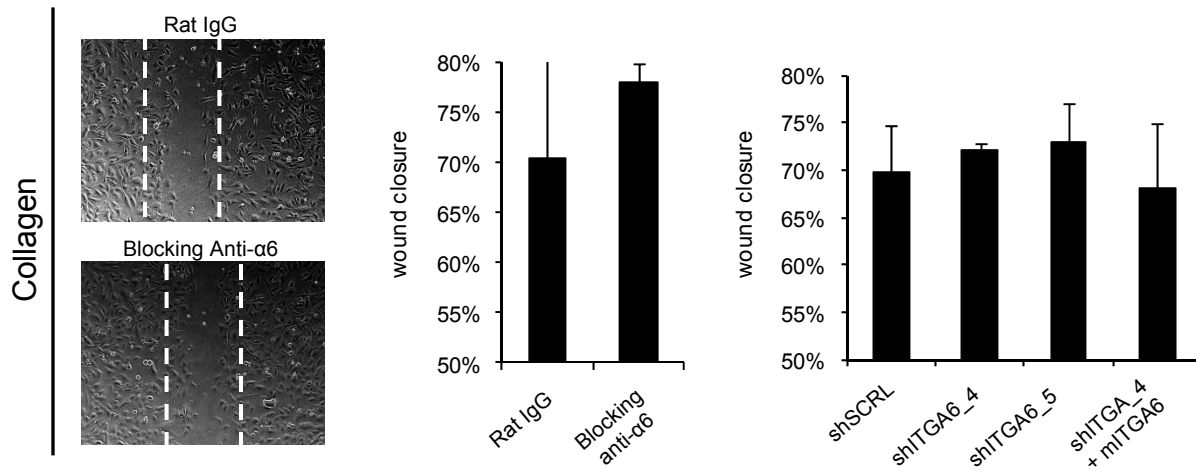


Supplemental Figure 4

A

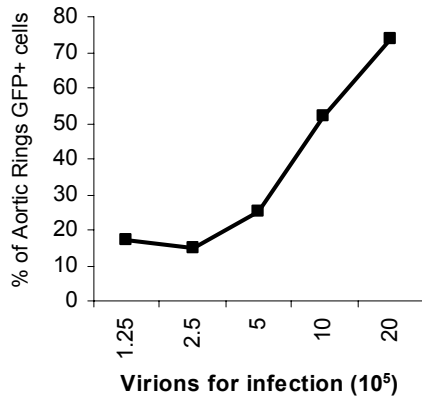


B

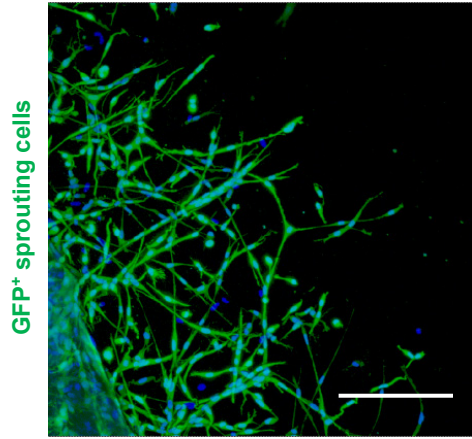


Supplemental Figure 5

A

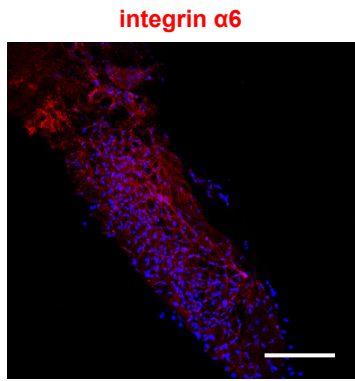


B

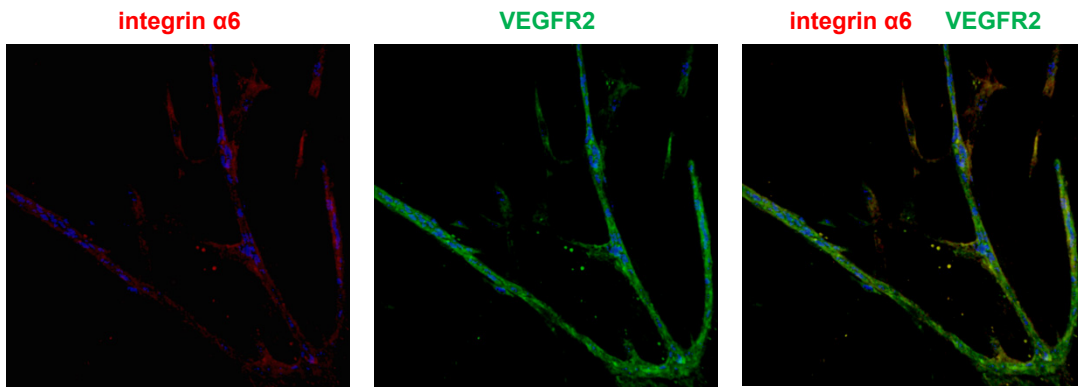


Supplemental Figure 6

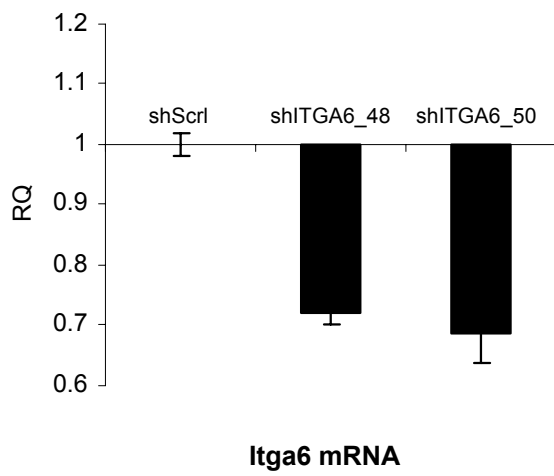
A



B

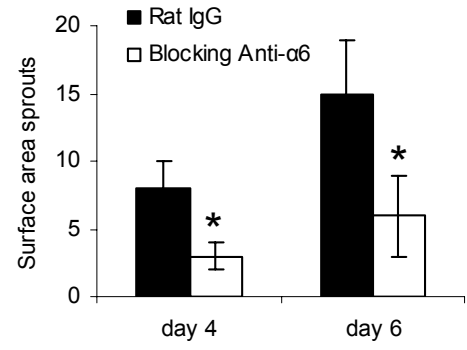
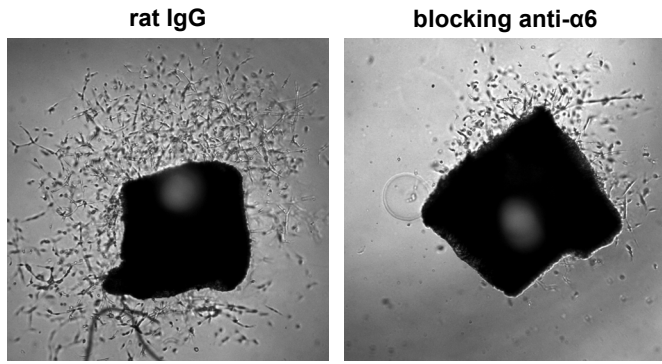


C



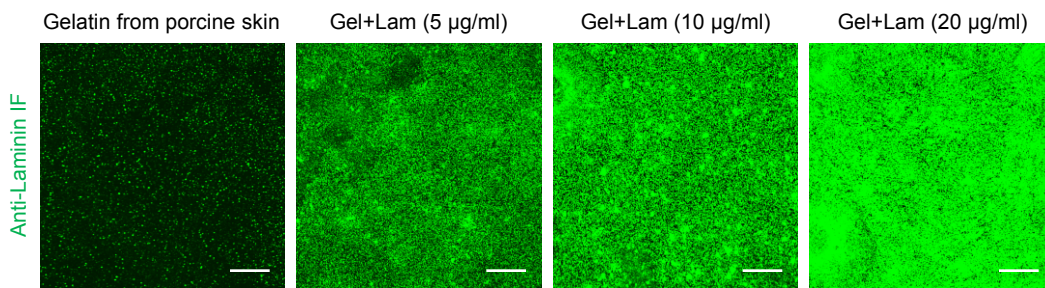
Supplemental Figure 7

A

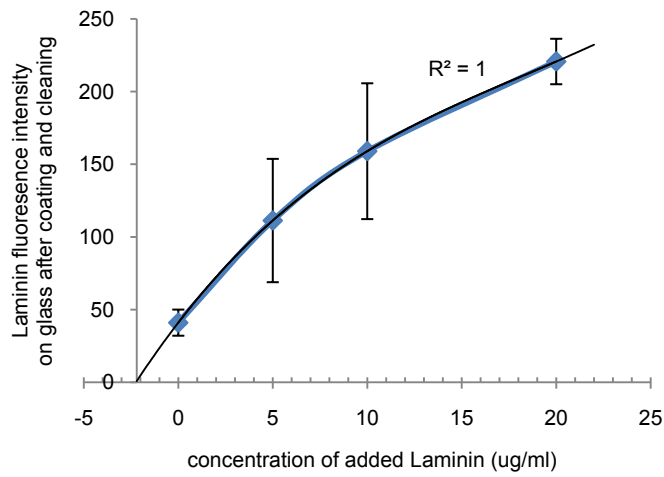


Supplemental Figure 8

A

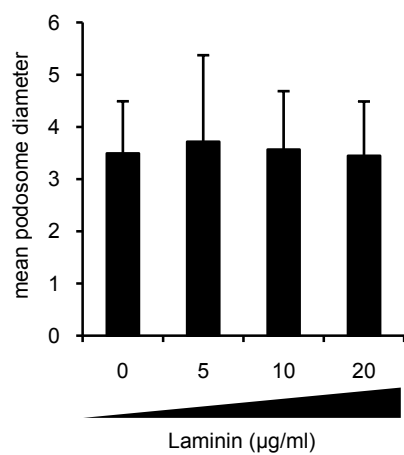


B

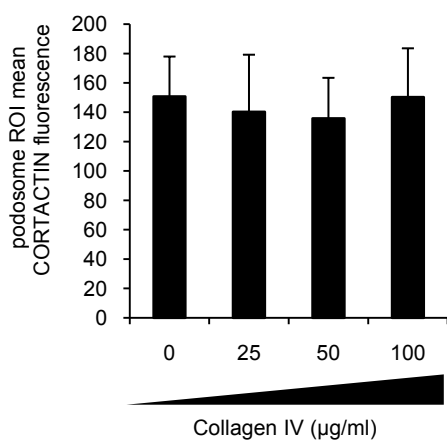


Supplemental Figure 9

A

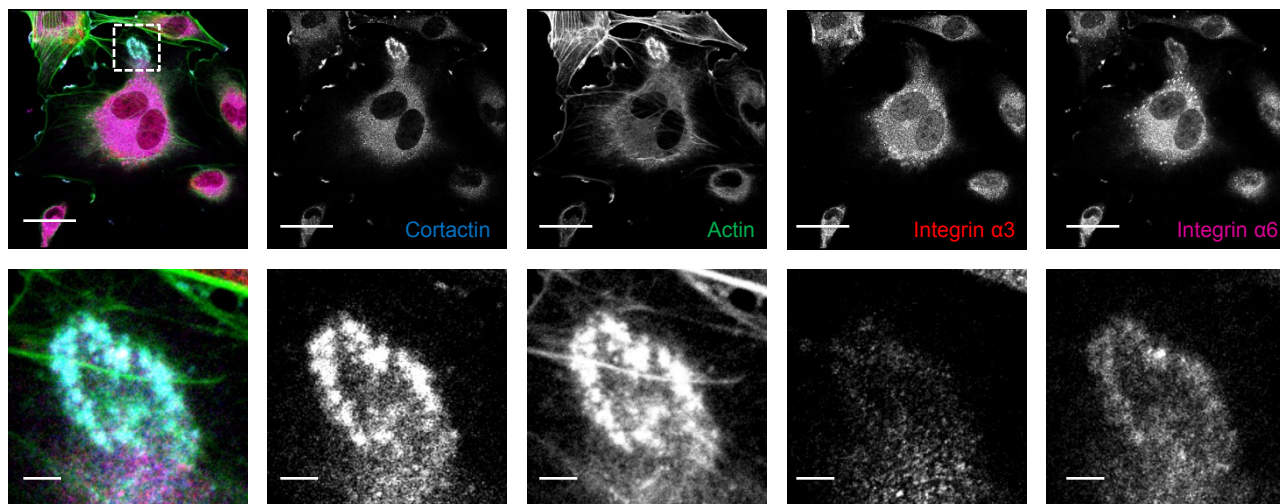


B

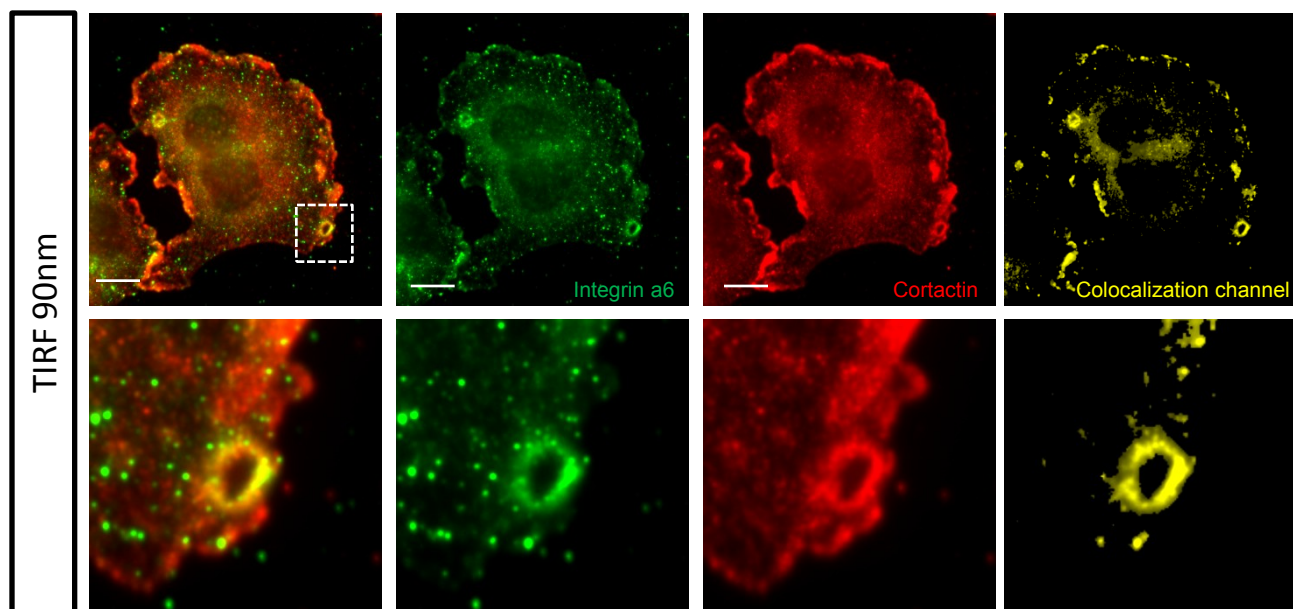


Supplemental Figure 10

A

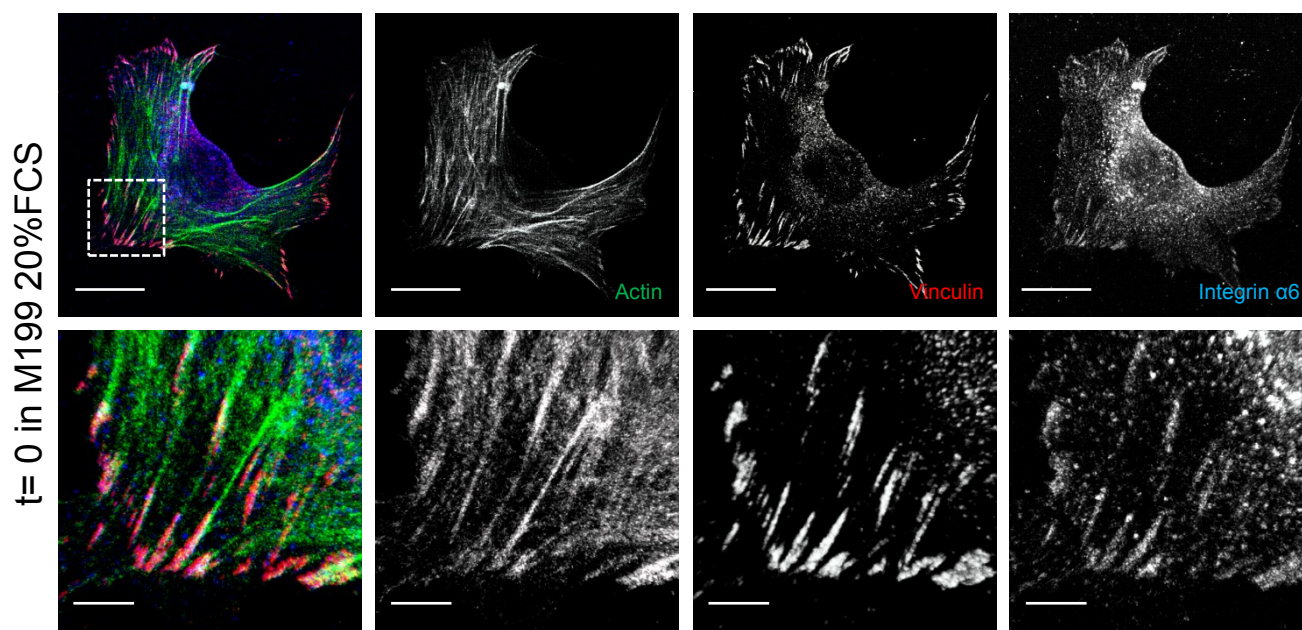


B

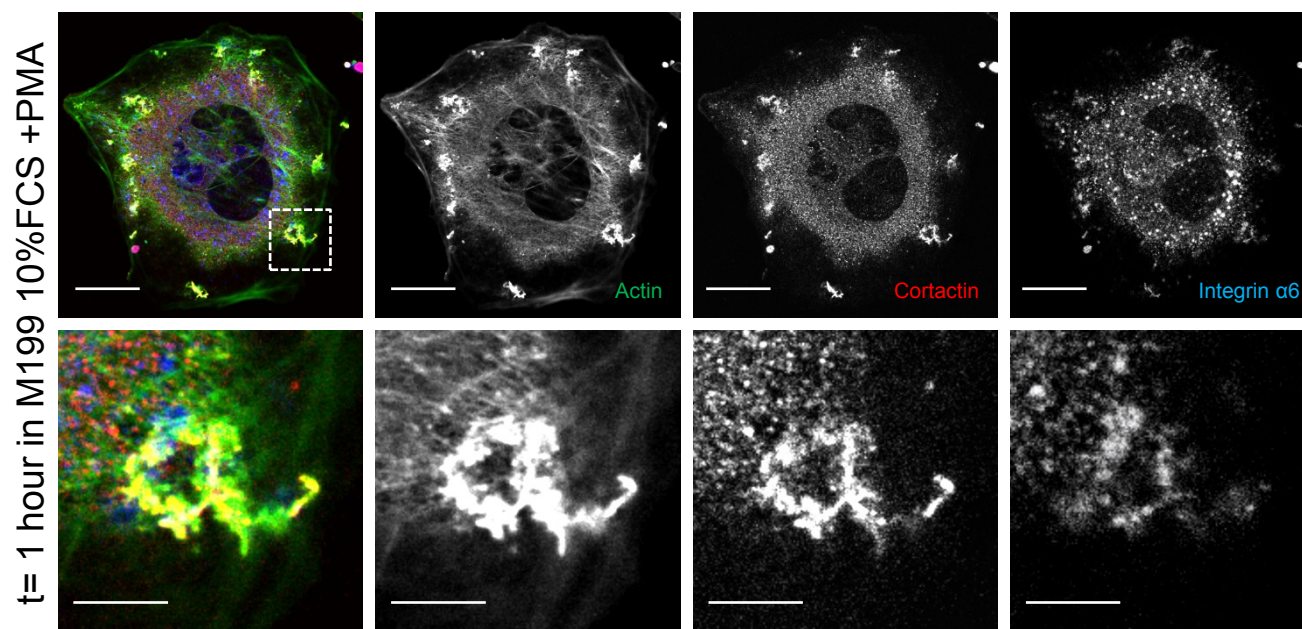


Supplemental Figure 11

A



B



SUPPLEMENTARY FIGURE LEGENDS

Figure S1. Membrane and total integrins quantification – EC, unstimulated or treated for 24h or 48h with VEGF-A or FGF2, were biotinylated and lysed. (a-b) $\alpha 6$ integrin was immunoprecipitated, and detected with streptavidin. (c) The same lysates were analyzed using anti- $\beta 1$ antibody. Graphs show mean relative pixel intensity \pm SD of 3 independent experiments.

Figure S2. Integrin $\alpha 6$ down-regulation by shRNA lentiviral-mediated transduction – (a) Levels of $\alpha 6$ integrin mRNA in ECs transduced with control shRNA (ShScr1) and ITGA6 specific shRNAs (shITGA6_4 and shITGA6_5). Relative quantification (RQ) in comparison with ShScr1 mRNA levels. mRNA levels are normalized to GAPDH protein. (b) Levels of $\alpha 6$ integrin surface expression in ECs transduced with control shRNA (ShScr1), ITGA6 specific shRNAs (shITGA6_4 and shITGA6_5) and ITGA6 specific shRNA with mouse ITGA6 cDNA (shITGA6_4+mItga6), evaluated by cytofluorimetric analysis; reported values are the average of percentages (%) of $\alpha 6$ -expressing cells.

Figure S3. Down-regulation or blocking of $\alpha 6$ integrin doesn't affect EC sprouting capability into type I collagen gel – (a) Spheroids of EC, transduced with control shRNA (ShScr1) and ITGA6 specific shRNAs (shITGA6_4, shITGA6_5), were embedded in collagen gel in the absence or presence of VEGF-A and FGF2, and observed after 48h. Photographs are representative

of 3 different experiments with more than 10 spheroids each. Graph shows means of quantification of sprouting length per spheroid. \pm SD of 3 different experiments with more than 10 spheroids each. (b) Spheroids of EC, treated with rat IgG or $\alpha 6$ integrin blocking Ab, were embedded in collagen or BME gel in the absence or presence of VEGF-A, and observed after 24h. Photographs are representative of 3 different experiments with more than 10 spheroids each.

Figure S4. Adhesion capability and motility of ECs down-regulated or inhibited for $\alpha 6$ integrin. (a) Effect of $\alpha 6$ integrin down-regulation on adhesion of ECs onto different extracellular matrix. The mean absorbance values \pm SD obtained at 595 nm were from triplicate wells containing crystal violet stained cells. Cells were incubated for 30 min with medium in the presence of VEGF-A and FGF2. (b) ECs, transduced as indicated or treated with blocking antibody, were plated on collagen in the presence of VEGF-A and FGF2 followed by wounding. White broken lines delimitate the initial positions of wounds. Graphs show mean percentage of wound closure after 7 hours of migration \pm SD of 2 independent experiments, each in triplicate.

Figure S5. Aortic ring lentiviral transduction efficiency. (a) Efficiency of lentivirus infection evaluated with cytofluorimetric analysis of GFP⁺ cells after disaggregation of matrix gel. Reported values are average percentages of 5 mouse Aortic Rings infected with the indicated amount of virions. (b) Confocal image of a representative 5-day old mouse aortic ring transduced with pLKO.1-GFP (scale bar: 150 μ m).

Figure S6. ITGA6 expression and shRNA-mediated silencing in mouse aortic rings assay. (a) Immunostaining of whole-mounted mouse aorta for integrin $\alpha 6$ (red) and nuclear staining with DAPI (blue). (b) Whole-mount mouse aortic ring immunostaining of angiogenic outgrowth into matrix gel. VEGFR2 (green) and integrin $\alpha 6$ (red) and nuclear staining with DAPI (blue). (c) Analysis of ITGA6 silencing efficiency with qRT-PCR. Relative quantification (RQ) in comparison with ShScr1 mRNA levels of infected Mouse Aortic Rings. mRNA levels are normalized to TATA-binding box protein.

Figure S7. $\alpha 6$ integrin promotes angiogenesis into basement membrane extract gel. (a) Aortic rings were observed after 4 and 6 days in BME gel. Rat IgG and GOH3 blocking antibody were applied before gel solidification and administrated in medium with a final concentration of 10 mg/ml. Photographs of day 6 are representatives of 3 experiments. Sprouting angiogenesis was quantified as tubular areas. Values are average \pm SD of 3 independent experiments, each in quintuplicate and from different mice (* $P < 0.05$ versus control rat IgG treatment).

Figure S8. Laminin concentration of 1% porcine gelatin for coating. (a) Representative confocal images of coated glass coverslips, stained with anti-Laminin Ab (green) (scale bar: 20 μm). (b) Quantification of laminin concentration present in gelatin coating of coverslips. The intersection of trend line ($R^2=1$) with x-axis shows the hypothetical concentration of laminin in gelatin film without hexogen addition of laminin.

Figure S9. Podosomal diameter and cortactin localization in EC seeded on laminin or type-IV collagen. (a) Quantification of mean diameter of podosomal actin-cortactin ring of EC seeded on growing concentrations of laminin. Columns, mean of three independent experiments, six cells per experimental point each experiment; bar, SD. (b) Quantification of cortactin in podosome ROIs of

EC seeded on growing concentrations of type-IV collagen. Columns, mean fluorescence detected in podosomes ROI, identified with F-actin-cortactin colocalization, of three independent experiments, six cells per experimental point each experiment; bar, SD.

Figure S10. $\alpha 3$ integrin is not recruited in podosome, while integrin $\alpha 6$ is localized in zones of close adhesion to the substratum. (a) Confocal images of a representative EC, stained with anti-cortactin (blue), phalloidin (green), anti-integrin $\alpha 3$ (red) and anti-integrin $\alpha 6$ (magenta); (bar, 20 μm). The square dotted line (top) is enlarged in the bottom (bar, 2 μm). (b) TIRF microscopy images of a representative EC, stained with anti-integrin $\alpha 6$ (green), anti-cortactin (red) and related colocalization channel (yellow); (bar, 10 μm). The square dotted line (top) is enlarged in the bottom.

Figure S11. $\alpha 6$ integrin is actively translocated from pre-existing cellular adhesion compartment. (a) Confocal images of a representative EC at T=0 (well-formed focal adhesions), stained with phalloidin (green), anti-vinculin (red) – marker of focal adhesions – and anti-integrin $\alpha 6$ (blue); (bar, 20 μm). The square dotted line (top) is enlarged in the bottom (bar, 5 μm). (b) Confocal images of a representative EC after 1 hour with PMA-stimulation (podosome formation), stained with phalloidin (green), anti-cortactin (red) – podosomal marker – and anti-integrin $\alpha 6$ (blue); (bar, 20 μm). The square dotted line (top) is enlarged in the bottom (bar, 5 μm).

REFERENCES

1. Phng, L.K. and H. Gerhardt, *Angiogenesis: a team effort coordinated by notch*. Dev Cell, 2009. **16**(2): p. 196-208.
2. Block, M.R., et al., *Podosome-type adhesions and focal adhesions, so alike yet so different*. Eur J Cell Biol, 2008. **87**(8-9): p. 491-506.
3. Conway, E.M., D. Collen, and P. Carmeliet, *Molecular mechanisms of blood vessel growth*. Cardiovasc Res, 2001. **49**(3): p. 507-21.
4. Kalluri, R., *Basement membranes: structure, assembly and role in tumour angiogenesis*. Nat Rev Cancer, 2003. **3**(6): p. 422-33.
5. Risau, W., *Mechanisms of angiogenesis*. Nature, 1997. **386**(6626): p. 671-4.
6. Paulsson, M., *Basement membrane proteins: structure, assembly, and cellular interactions*. Crit Rev Biochem Mol Biol, 1992. **27**(1-2): p. 93-127.
7. Vracko, R., D. Thorning, and T.W. Huang, *Basal lamina of alveolar epithelium and capillaries: quantitative changes with aging and in diabetes mellitus*. Am Rev Respir Dis, 1979. **120**(5): p. 973-83.
8. Sund, M., L. Xie, and R. Kalluri, *The contribution of vascular basement membranes and extracellular matrix to the mechanics of tumor angiogenesis*. APMIS, 2004. **112**(7-8): p. 450-62.
9. Alitalo, K., et al., *Extracellular matrix components synthesized by human amniotic epithelial cells in culture*. Cell, 1980. **19**(4): p. 1053-62.
10. Hynes, R.O., *Integrins: bidirectional, allosteric signaling machines*. Cell, 2002. **110**(6): p. 673-87.
11. Brooks, P.C., R.A. Clark, and D.A. Cheresh, *Requirement of vascular integrin alpha v beta 3 for angiogenesis*. Science, 1994. **264**(5158): p. 569-71.
12. Drake, C.J., D.A. Cheresh, and C.D. Little, *An antagonist of integrin alpha v beta 3 prevents maturation of blood vessels during embryonic neovascularization*. J Cell Sci, 1995. **108 (Pt 7)**: p. 2655-61.
13. Bader, B.L., et al., *Extensive vasculogenesis, angiogenesis, and organogenesis precede lethality in mice lacking all alpha v integrins*. Cell, 1998. **95**(4): p. 507-19.
14. Hodivala-Dilke, K.M., et al., *Beta3-integrin-deficient mice are a model for Glanzmann thrombasthenia showing placental defects and reduced survival*. J Clin Invest, 1999. **103**(2): p. 229-38.
15. Reynolds, A.R., et al., *Stimulation of tumor growth and angiogenesis by low concentrations of RGD-mimetic integrin inhibitors*. Nat Med, 2009. **15**(4): p. 392-400.
16. Senger, D.R., et al., *Angiogenesis promoted by vascular endothelial growth factor: regulation through alpha1beta1 and alpha2beta1 integrins*. Proc Natl Acad Sci U S A, 1997. **94**(25): p. 13612-7.
17. Nikolopoulos, S.N., et al., *Integrin beta4 signaling promotes tumor angiogenesis*. Cancer Cell, 2004. **6**(5): p. 471-83.
18. Kennel, S.J., et al., *Sequence of a cDNA encoding the beta 4 subunit of murine integrin*. Gene, 1993. **130**(2): p. 209-16.
19. Georges-Labouesse, E., et al., *Absence of integrin alpha 6 leads to epidermolysis bullosa and neonatal death in mice*. Nat Genet, 1996. **13**(3): p. 370-3.
20. van der Neut, R., et al., *Epithelial detachment due to absence of hemidesmosomes in integrin beta 4 null mice*. Nat Genet, 1996. **13**(3): p. 366-9.

21. Linder, S., *The matrix corroded: podosomes and invadopodia in extracellular matrix degradation*. Trends Cell Biol, 2007. **17**(3): p. 107-17.
22. Zamir, E. and B. Geiger, *Molecular complexity and dynamics of cell-matrix adhesions*. J Cell Sci, 2001. **114**(Pt 20): p. 3583-90.
23. Buccione, R., J.D. Orth, and M.A. McNiven, *Foot and mouth: podosomes, invadopodia and circular dorsal ruffles*. Nat Rev Mol Cell Biol, 2004. **5**(8): p. 647-57.
24. Ridley, A.J., et al., *Cell migration: integrating signals from front to back*. Science, 2003. **302**(5651): p. 1704-9.
25. Van Haastert, P.J. and P.N. Devreotes, *Chemotaxis: signalling the way forward*. Nat Rev Mol Cell Biol, 2004. **5**(8): p. 626-34.
26. De Smet, F., et al., *Mechanisms of vessel branching: filopodia on endothelial tip cells lead the way*. Arterioscler Thromb Vasc Biol, 2009. **29**(5): p. 639-49.
27. Friedl, P. and D. Gilmour, *Collective cell migration in morphogenesis, regeneration and cancer*. Nat Rev Mol Cell Biol, 2009. **10**(7): p. 445-57.
28. Montell, D.J., *Morphogenetic cell movements: diversity from modular mechanical properties*. Science, 2008. **322**(5907): p. 1502-5.
29. Carmeliet, P. and M. Tessier-Lavigne, *Common mechanisms of nerve and blood vessel wiring*. Nature, 2005. **436**(7048): p. 193-200.
30. Horowitz, A. and M. Simons, *Branching morphogenesis*. Circ Res, 2008. **103**(8): p. 784-95.
31. Mazzone, M., et al., *Heterozygous deficiency of PHD2 restores tumor oxygenation and inhibits metastasis via endothelial normalization*. Cell, 2009. **136**(5): p. 839-51.
32. Bussolino, F., et al., *Hepatocyte growth factor is a potent angiogenic factor which stimulates endothelial cell motility and growth*. J Cell Biol, 1992. **119**(3): p. 629-41.
33. Korff, T. and H.G. Augustin, *Integration of endothelial cells in multicellular spheroids prevents apoptosis and induces differentiation*. J Cell Biol, 1998. **143**(5): p. 1341-52.
34. Moffat, J., et al., *A lentiviral RNAi library for human and mouse genes applied to an arrayed viral high-content screen*. Cell, 2006. **124**(6): p. 1283-98.
35. Roca, C., et al., *Hyperthermia inhibits angiogenesis by a plasminogen activator inhibitor 1-dependent mechanism*. Cancer Res, 2003. **63**(7): p. 1500-7.
36. Rottiers, P., et al., *TGFbeta-induced endothelial podosomes mediate basement membrane collagen degradation in arterial vessels*. J Cell Sci, 2009. **122**(Pt 23): p. 4311-8.
37. Linder, S. and M. Aepfelbacher, *Podosomes: adhesion hot-spots of invasive cells*. Trends Cell Biol, 2003. **13**(7): p. 376-85.
38. Tatin, F., et al., *A signalling cascade involving PKC, Src and Cdc42 regulates podosome assembly in cultured endothelial cells in response to phorbol ester*. J Cell Sci, 2006. **119**(Pt 4): p. 769-81.
39. Head, J.A., et al., *Cortactin tyrosine phosphorylation requires Rac1 activity and association with the cortical actin cytoskeleton*. Mol Biol Cell, 2003. **14**(8): p. 3216-29.
40. Zhan, X., et al., *Murine cortactin is phosphorylated in response to fibroblast growth factor-1 on tyrosine residues late in the G1 phase of the BALB/c 3T3 cell cycle*. J Biol Chem, 1993. **268**(32): p. 24427-31.
41. Zhan, X., et al., *Association of fibroblast growth factor receptor-1 with c-Src correlates with association between c-Src and cortactin*. J Biol Chem, 1994. **269**(32): p. 20221-4.
42. Tarone, G., et al., *Rous sarcoma virus-transformed fibroblasts adhere primarily at discrete protrusions of the ventral membrane called podosomes*. Exp Cell Res, 1985. **159**(1): p. 141-57.
43. Osiak, A.E., G. Zenner, and S. Linder, *Subconfluent endothelial cells form podosomes downstream of cytokine and RhoGTPase signaling*. Exp Cell Res, 2005. **307**(2): p. 342-53.
44. Adams, R.H. and K. Alitalo, *Molecular regulation of angiogenesis and lymphangiogenesis*. Nat Rev Mol Cell Biol, 2007. **8**(6): p. 464-78.

45. Silva, R., et al., *Integrins: the keys to unlocking angiogenesis*. *Arterioscler Thromb Vasc Biol*, 2008. **28**(10): p. 1703-13.
46. Davis, G.E. and D.R. Senger, *Endothelial extracellular matrix: biosynthesis, remodeling, and functions during vascular morphogenesis and neovessel stabilization*. *Circ Res*, 2005. **97**(11): p. 1093-107.
47. Gerhardt, H., et al., *VEGF guides angiogenic sprouting utilizing endothelial tip cell filopodia*. *J Cell Biol*, 2003. **161**(6): p. 1163-77.
48. Jakobsson, L., et al., *Endothelial cells dynamically compete for the tip cell position during angiogenic sprouting*. *Nat Cell Biol*, 2010. **12**(10): p. 943-53.